Electronic Supplementary Material (ESI) for New Journal of Chemistry.
This journal is © The Royal Society of Chemistry and the Centre National de la Recherche Scientifique 2021

Studies of novel trifluoromethyl ketone containing hydrazone molecular photoswitches in solution and in the solid state

Gianluca Accorsi,*[a]Agostina-Lina Capodilupo[a], Rosa María Claramunt[b], Guy J. Clarkson[c], A. Farrán [b]*, Francesco G. Gatti[d], Salvador León[e] and Silvia Venturi.[d]

[a]*CNR NANOTEC - Institute of Nanotechnology c/o Campus Ecotekne, University of Salento, Via Monteroni, 73100 Lecce, Italy.*
[b]*Departamento de Química Orgánica y Bio-Orgánica, Facultad de Ciencias, Universidad Nacional de Educación a Distancia, Senda del Rey, 4, E-28040 Madrid, Spain*
[c]*Chemistry Department, University of Warwick, Library Rd. Coventry CV4 7AL United Kingdom*
[d]*Dipartimento di Chimica, Materiali ed Ingegneria Chimica "Giulio Natta", Politecnico di Milano, Via Mancinelli 7, 20131 Milano, Italy.*
[e]*Departamento de Ingeniería Química, Universidad Politécnica de Madrid, ETSIIM, José Gutiérrez Abascal 2, 28006 Madrid, Spain*

1. **Photophysical data** ____ **3**
2. **NMR Spectroscopy** ____ **10**
3. **X-Ray Analysis** ____ **25**
4. **DFT calculations** ____ **35**
5. **Kinetic studies of back thermal isomerization** ____ **37**
6. **References** ____ **46**

1. Photophysical data

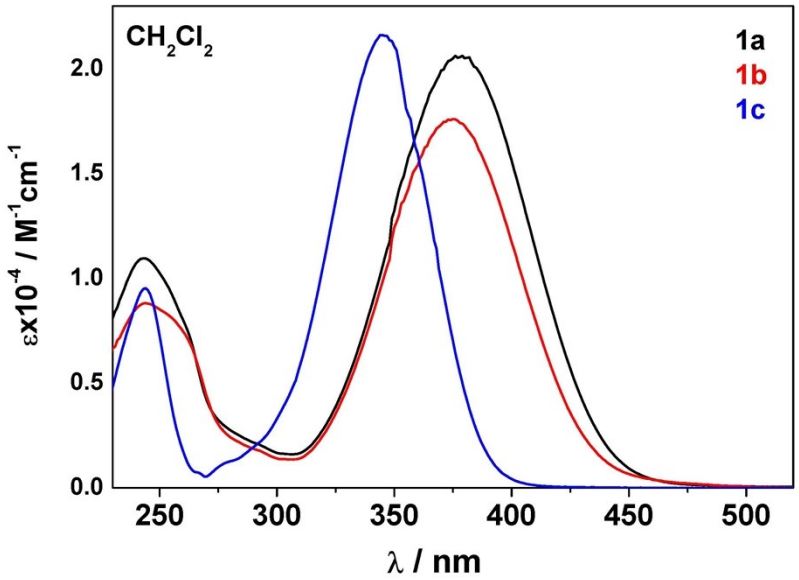

Fig.ESI1 Absorption profiles of (*E*)-**1a** (black), (*E*)-**1b** (red) and (*E*)-**1c** (blue) in CH_2Cl_2 at room temperature.

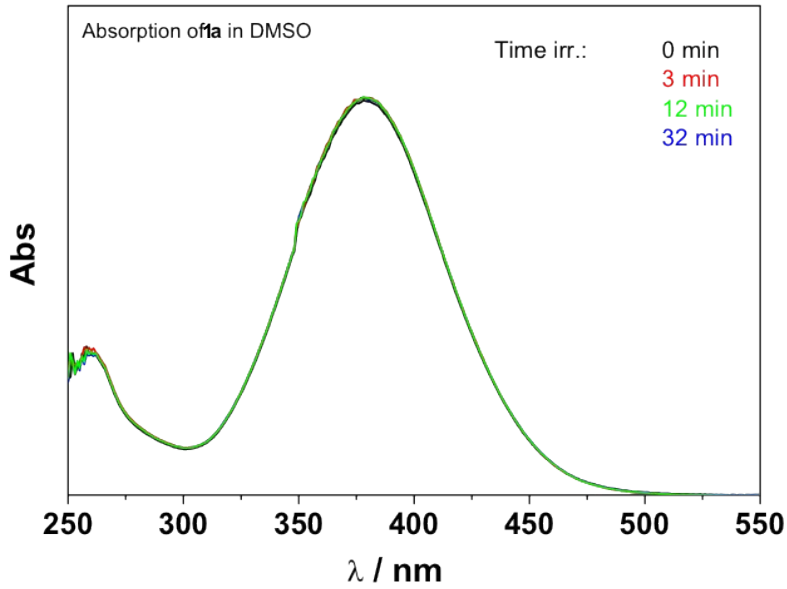

Fig.ESI2 Absorption profiles of (*E*)-**1a** in DMSO at room temperature under different irradiation times at 350 nm (λ_{IRR}: 5 microwatt/mm2).

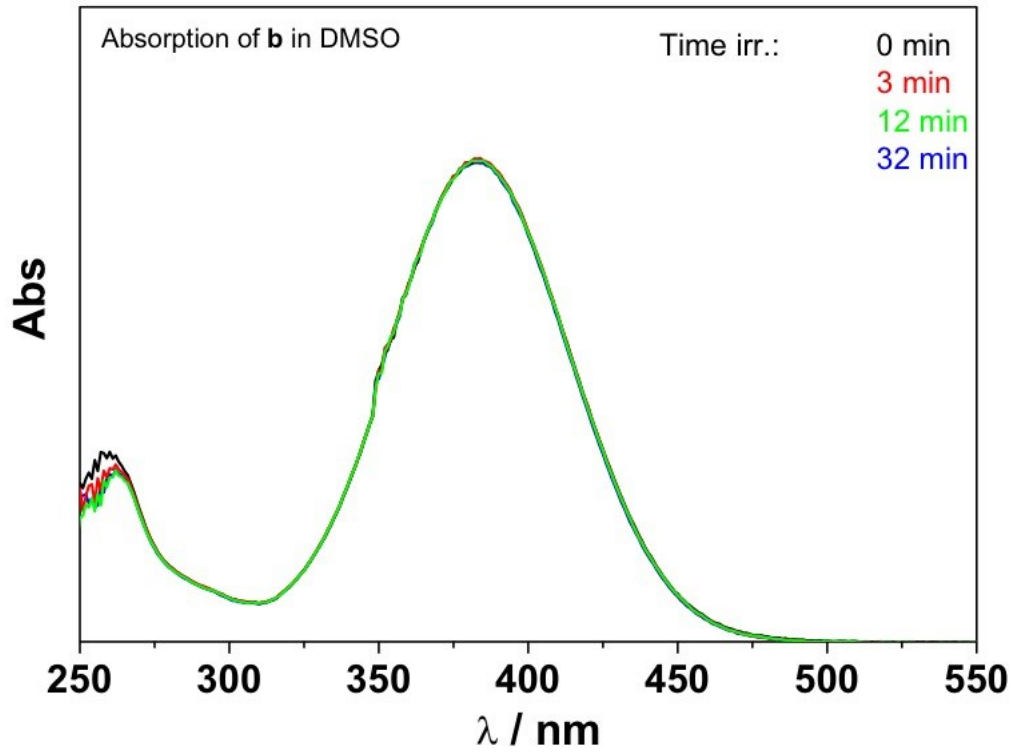

Fig.ESI3 Absorption profiles of (*E*)-**1b** in DMSO at room temperature under different irradiation times at 350 nm (λ_{IRR}: 5 microwatt/mm^2).

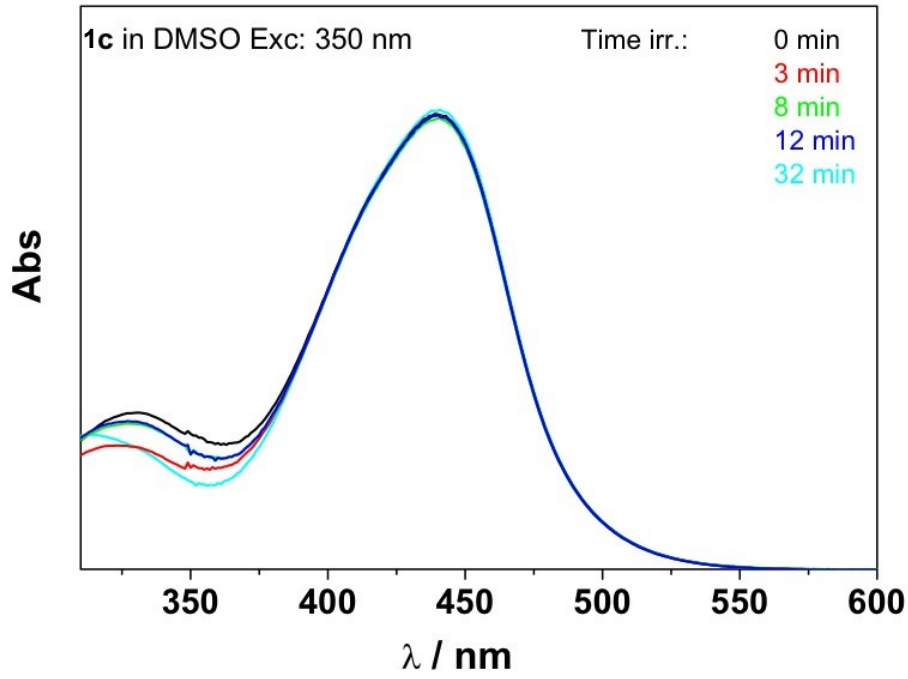

Fig. ESI4. Absorption profiles of **(*E*)-1c** in DMSO at room temperature under different irradiation times at 350 nm (λ_{IRR}: 5 microwatt/mm^2).

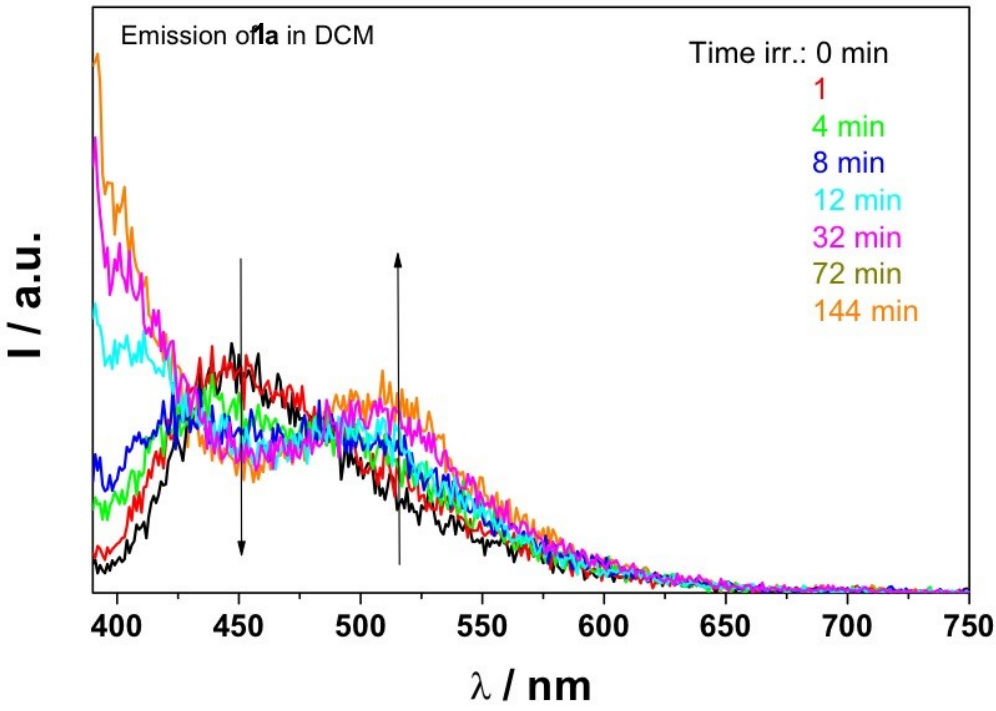

Fig. ESI5 Emission profiles of (*E*)-**1a** in CH_2Cl_2 at room temperature under different irradiation times at 350 nm (λ_{IRR}: 5 microwatt/mm^2).

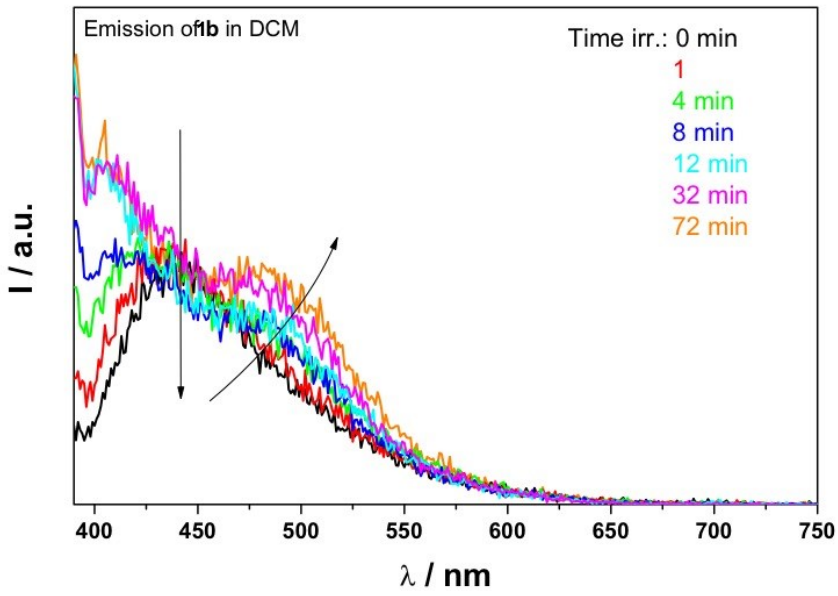

Fig.ESI6 Emission profiles of (*E*)-**1b** in CH_2Cl_2 at room temperature under different irradiation times at 350 nm (λ_{IRR}: 5 microwatt/mm^2).

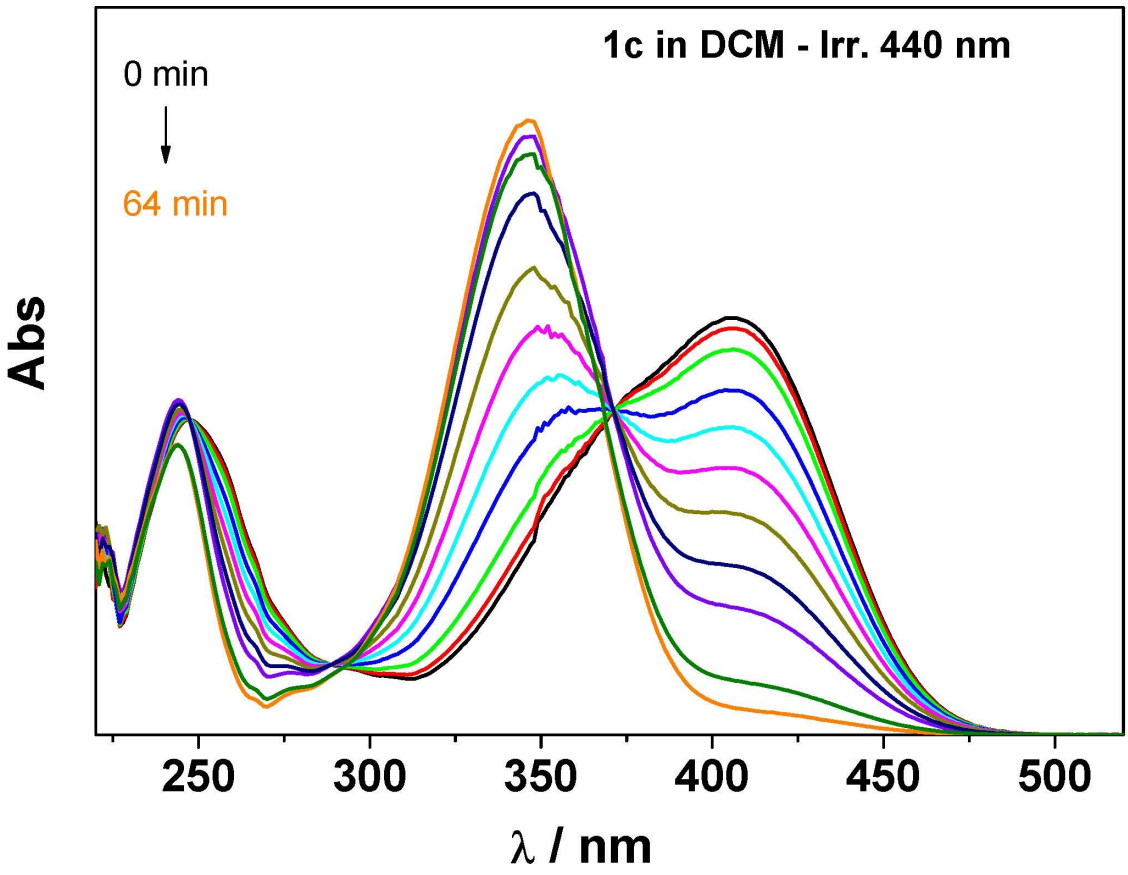

Fig. ESI7. Absorption profiles of (*E*)-**1c** in CH_2Cl_2 at room temperature under different irradiation times at 440 nm (λ_{IRR}: 23 microwatt/mm^2).

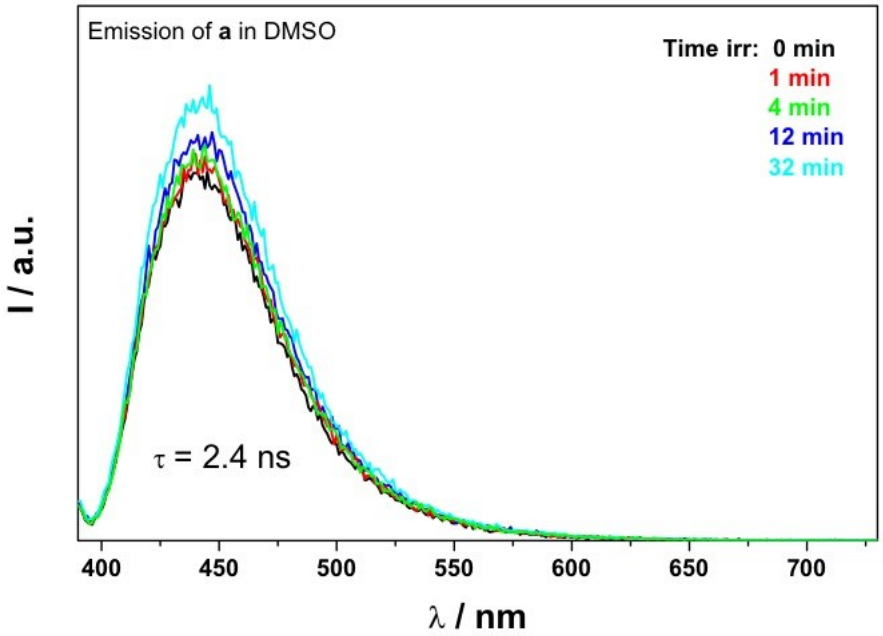

1 1

Fig. ESI8. Emission profiles of (*E*)-**1a** in DMSO at room temperature under different irradiation times at 350 nm (λ_{IRR}: 5 microwatt/mm^2).

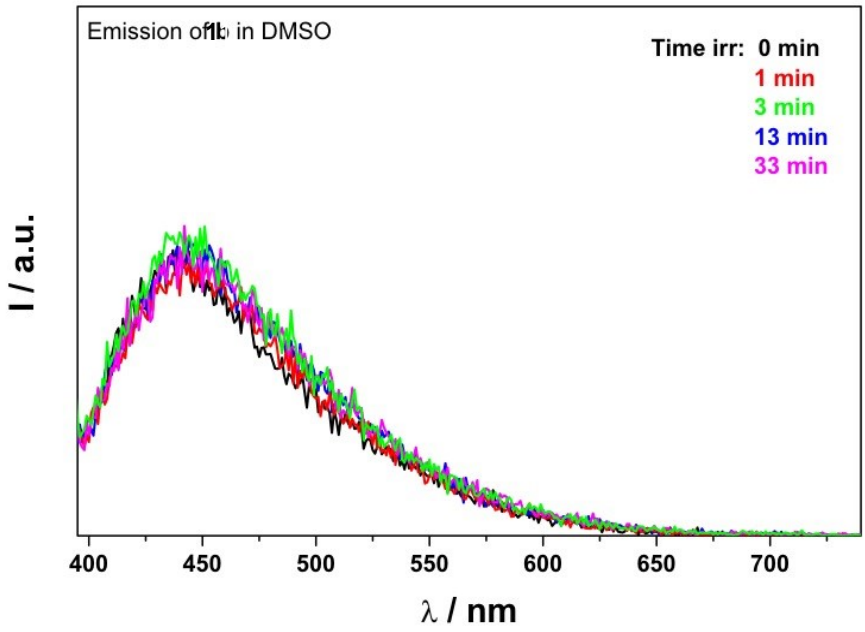

Fig. ESI9. Emission profiles of (*E*)-**1b** in DMSO at room temperature under different irradiation times at 350 nm (λ_{IRR}: 5 microwatt/mm^2).

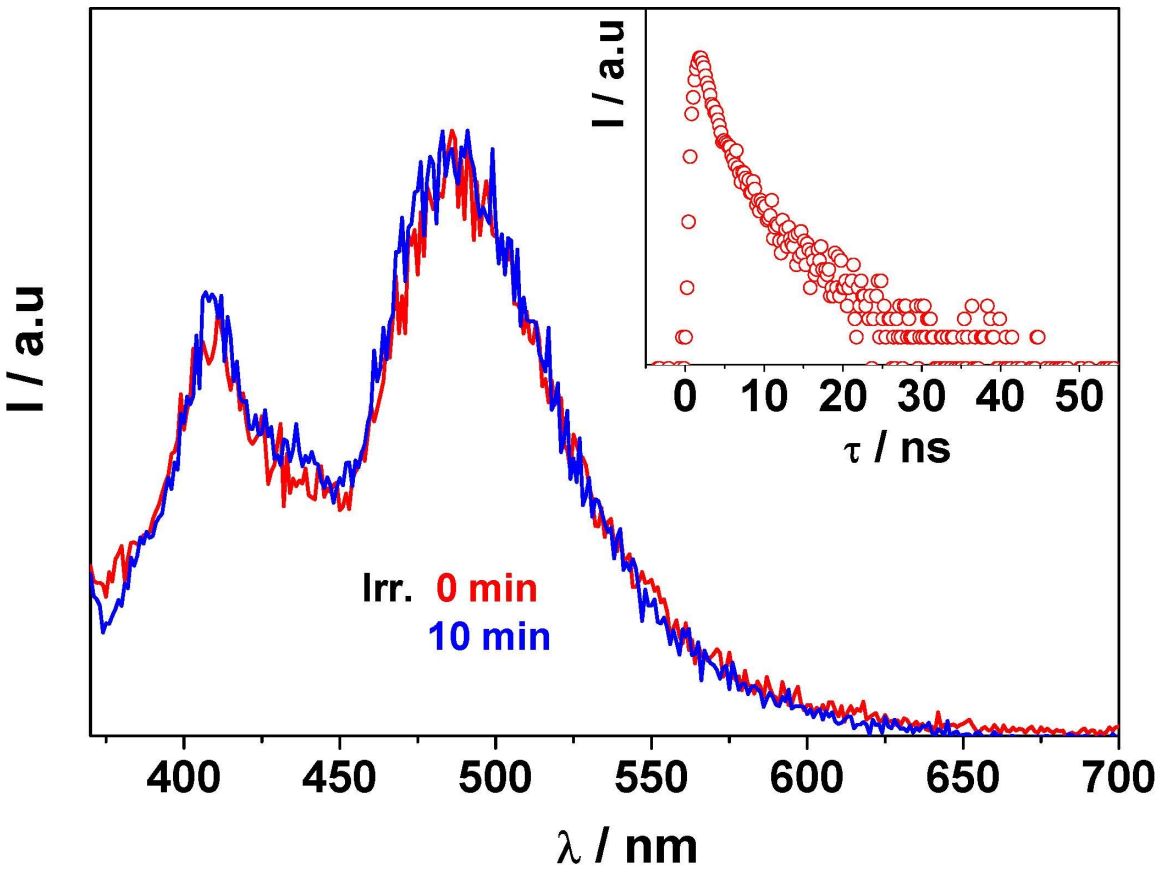

Fig. ESI9-b. Emission profiles (main window) and corresponding lifetime decay (Inset at t = 0) of (E)-1c in DMSO at room temperature after 10 min irradiation at 350 nm (red line, λ_{IRR}: 5 microwatt/mm^2) and no irradiation (blue line).

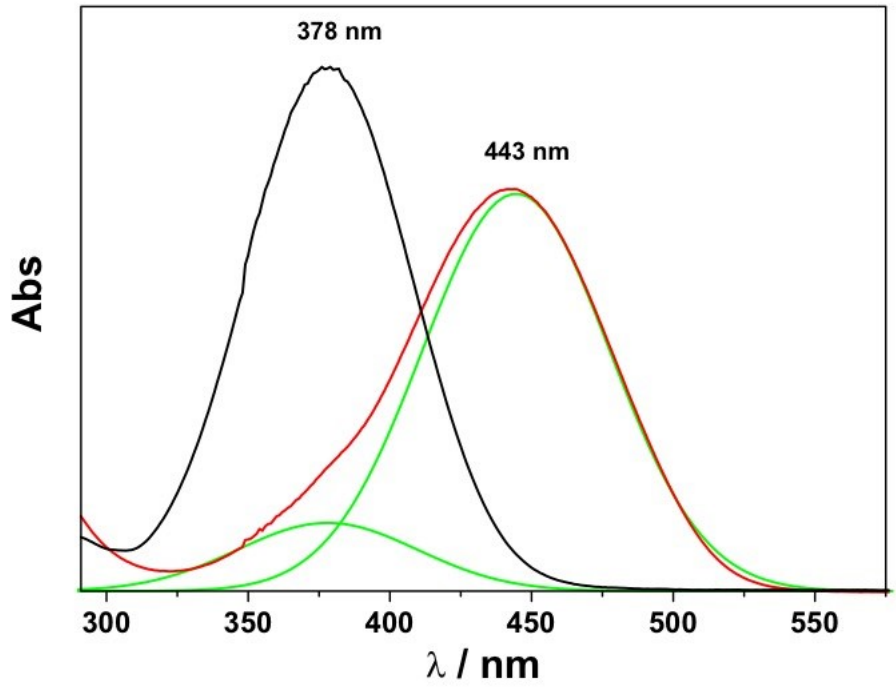

Fig. ESI10. Decovonluted spectra of **1a** in CH_2Cl_2. (Initial profile = black line; final profile = redline).

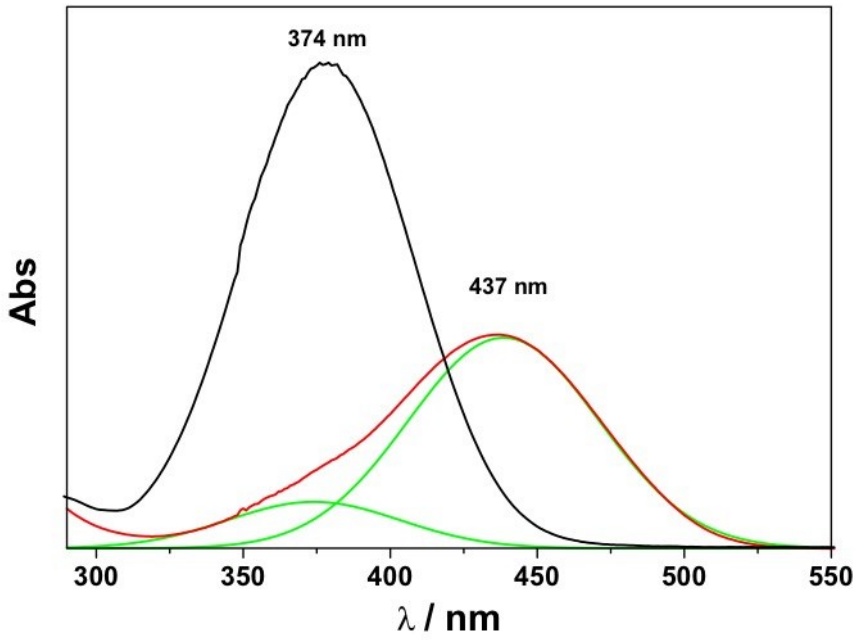

Fig. ESI11. Decovonluted spectra of **1b** in CH_2Cl_2. (Initial profile = black line; final profile = redline).

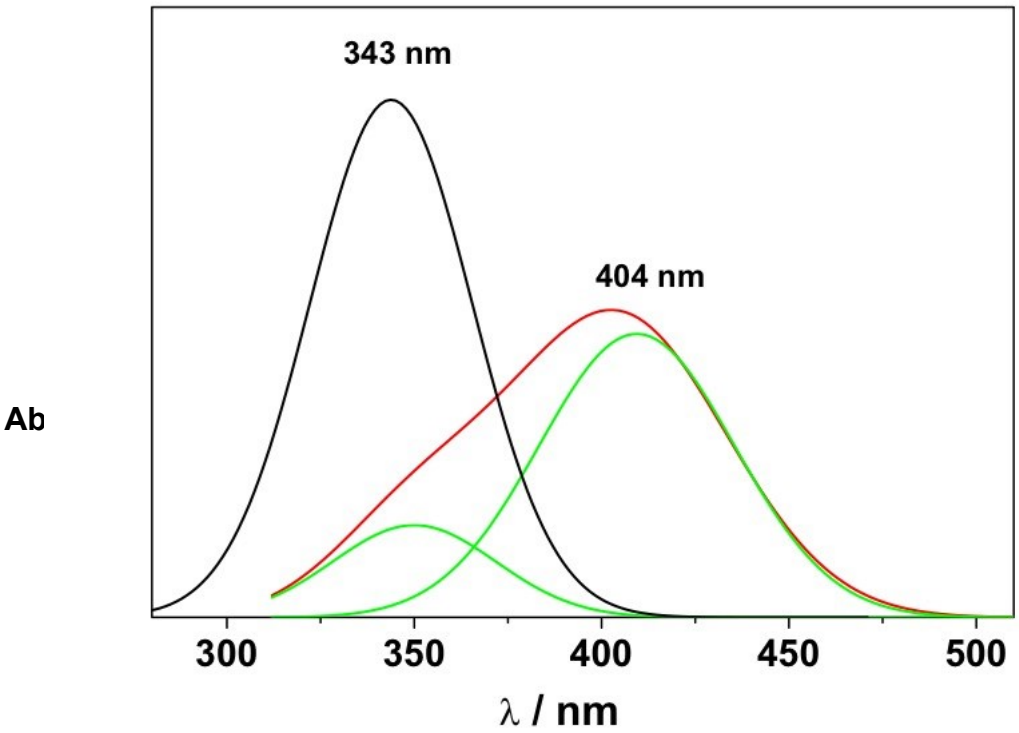

Fig. ESI12. Decovonluted spectra of **1c** in CH_2Cl_2. (Initial profile = black line; final profile = redline)

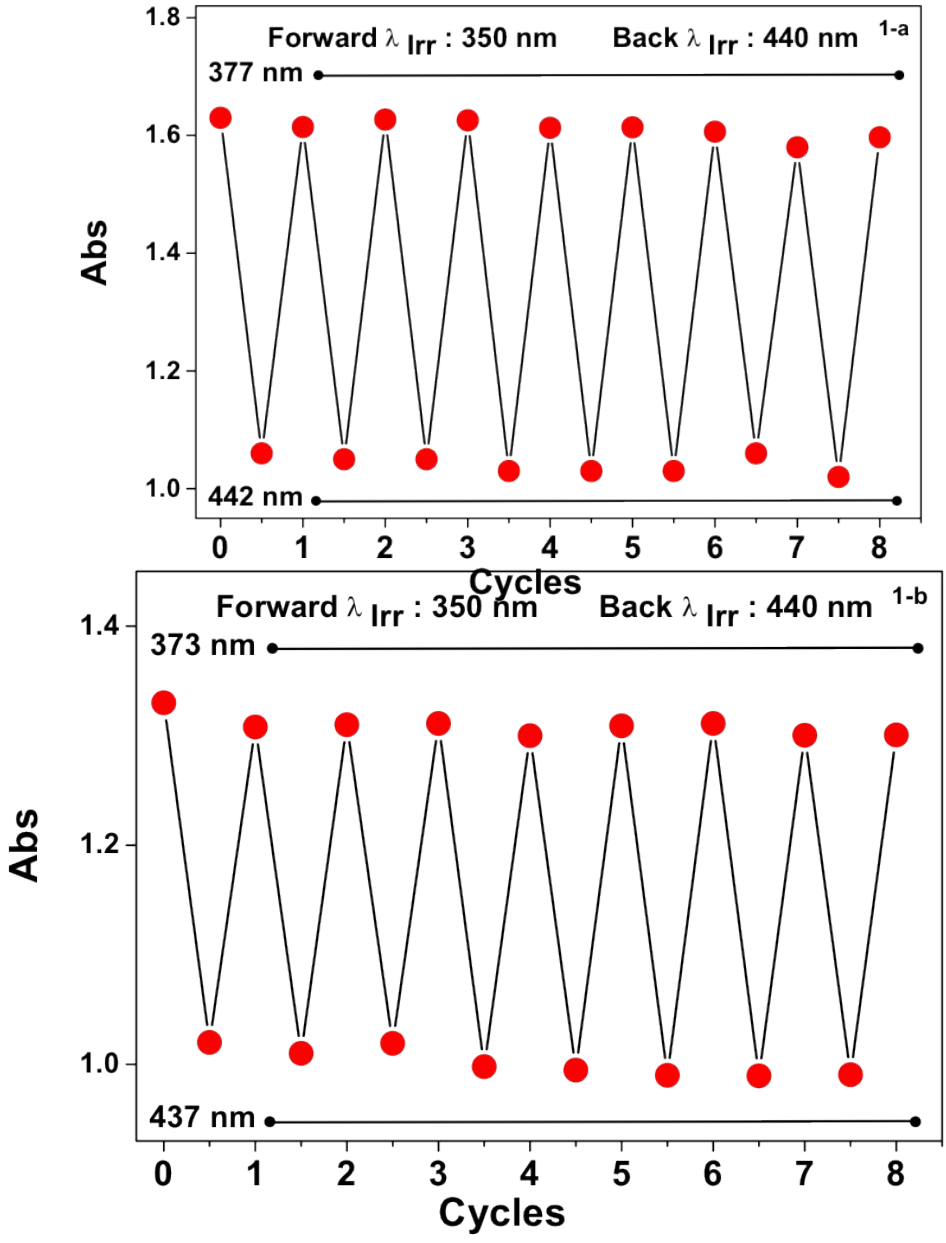

Fig. ESI13. Photocycling for **1a**

Fig. ESI14. Photocycling for **1b**

2. NMR Spectroscopy

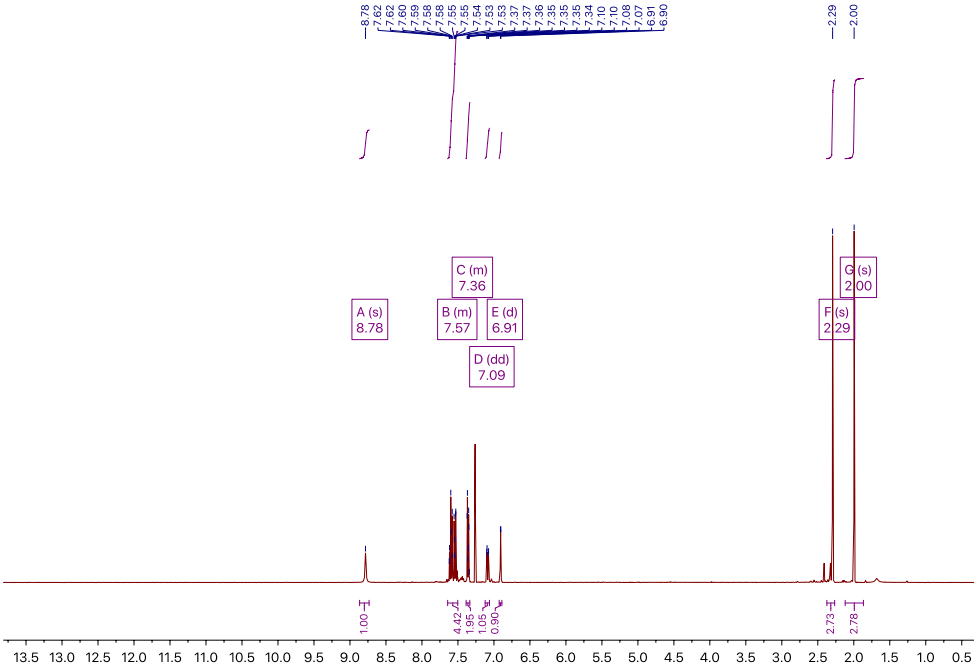

Fig. ESI15. 400 MHz ^{1}H NMR of (***E)*-1a.**

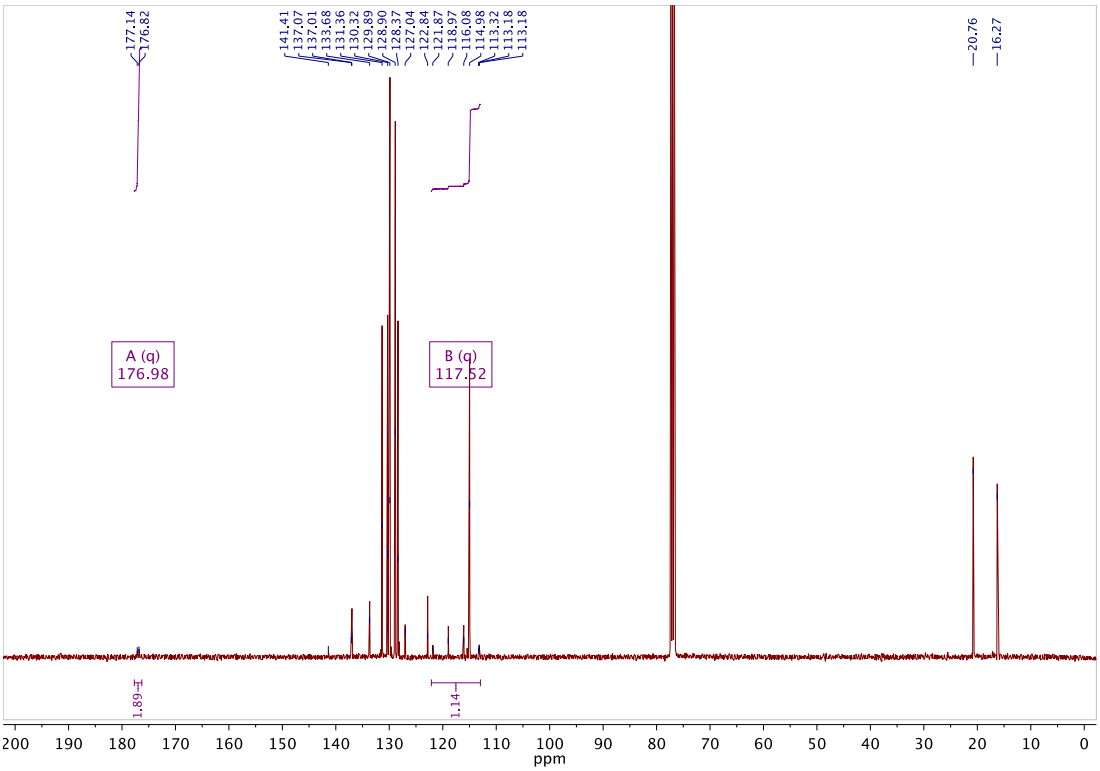

Fig ESI16 100.62 MHz ^{13}C NMR of (*E*)-**1a.**

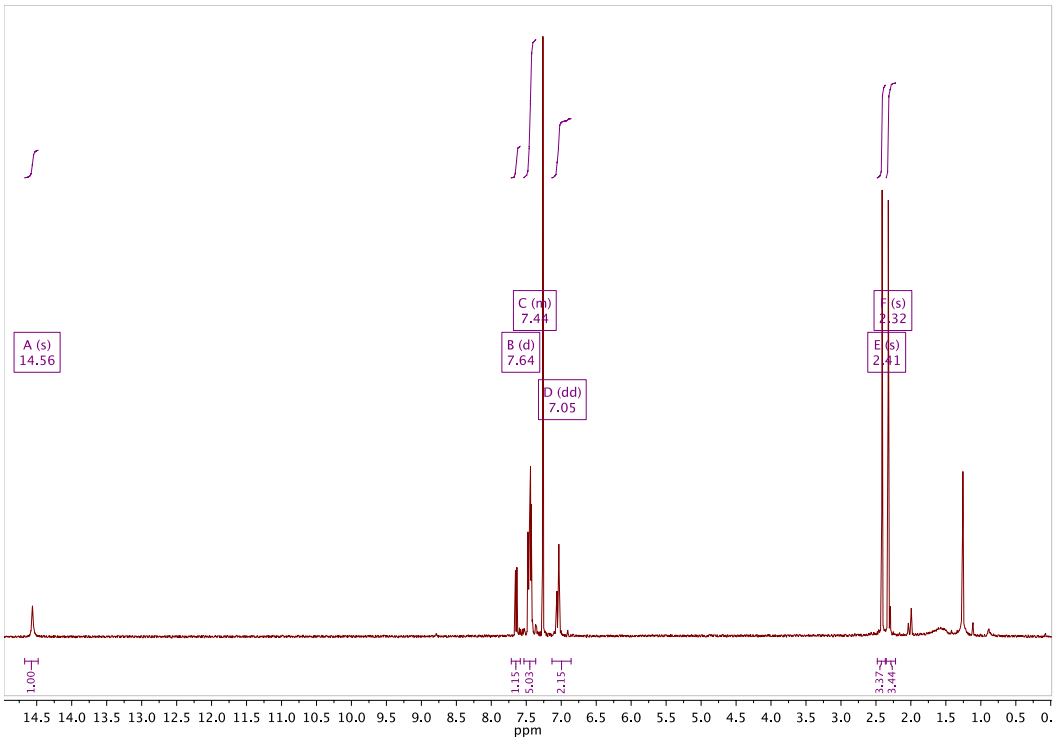

Fig. ESI17. 400.13 MHz ^{1}H NMR of (*Z*)-**1a.**

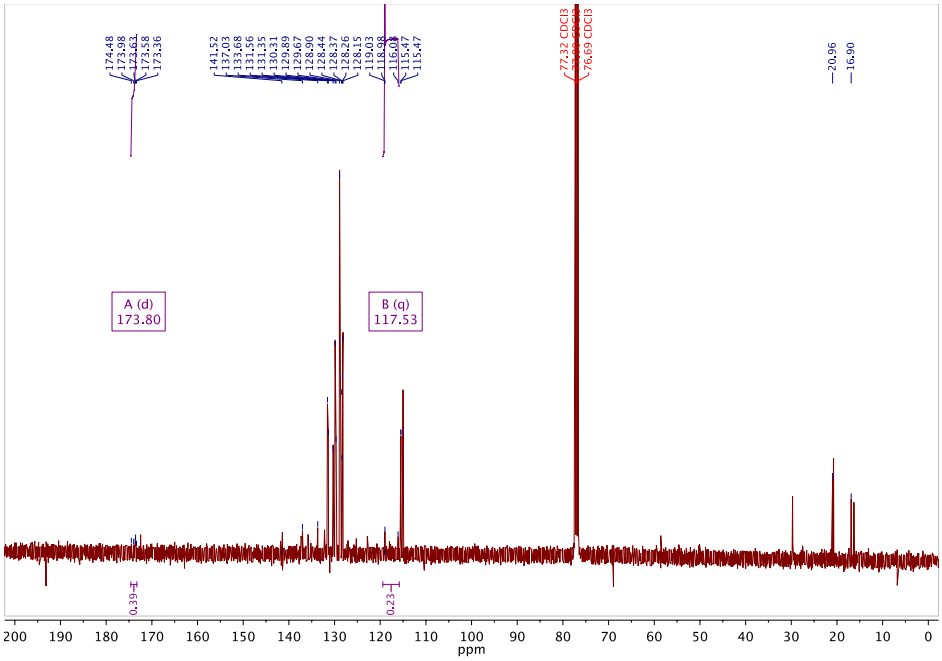

Fig ESI18. 100.62 MHz ^{13}C NMR of **(*E*)-1a.**

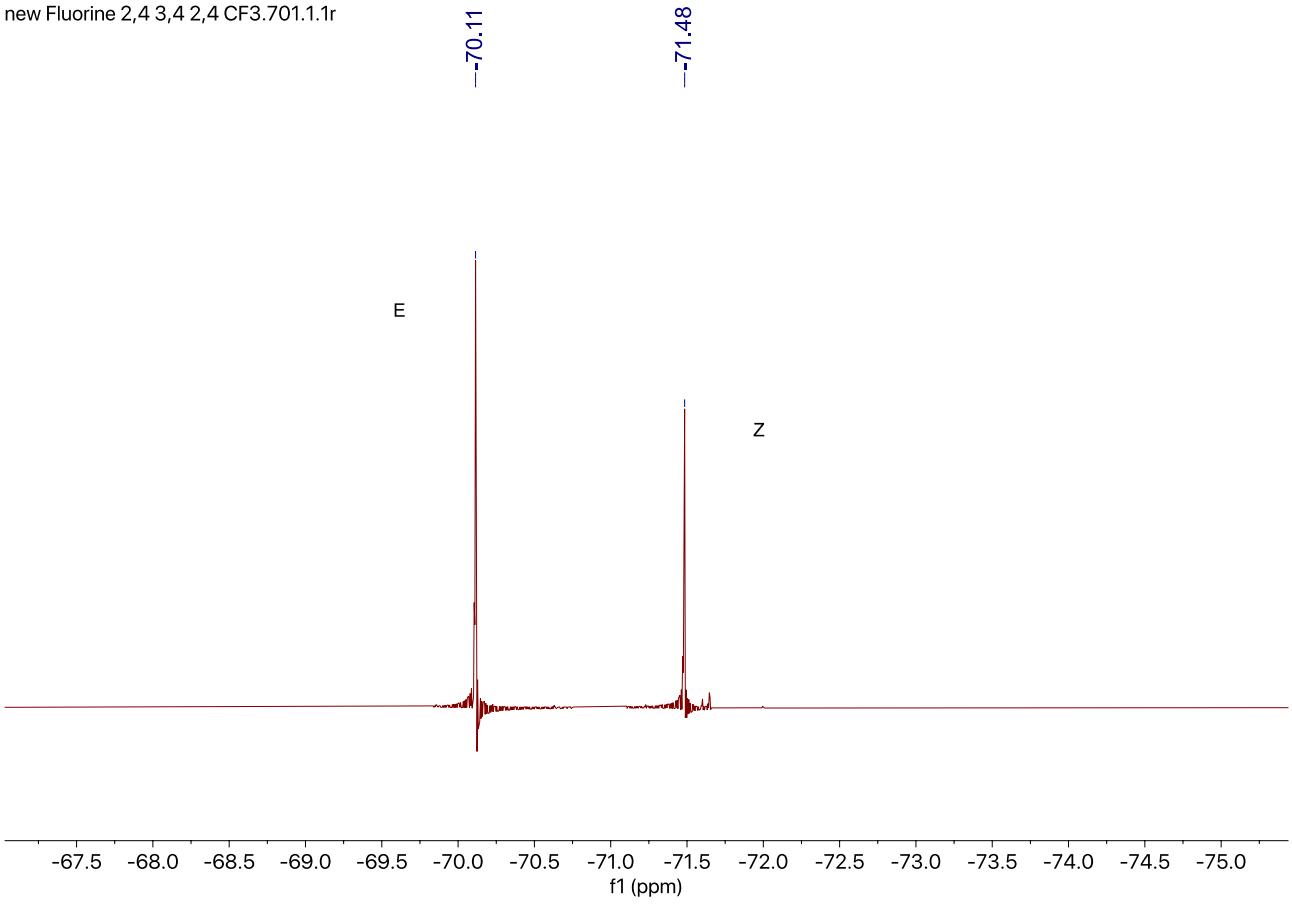

Fig. ESI19. 373.73 MHz ^{19}F NMR of **1a** isomers.

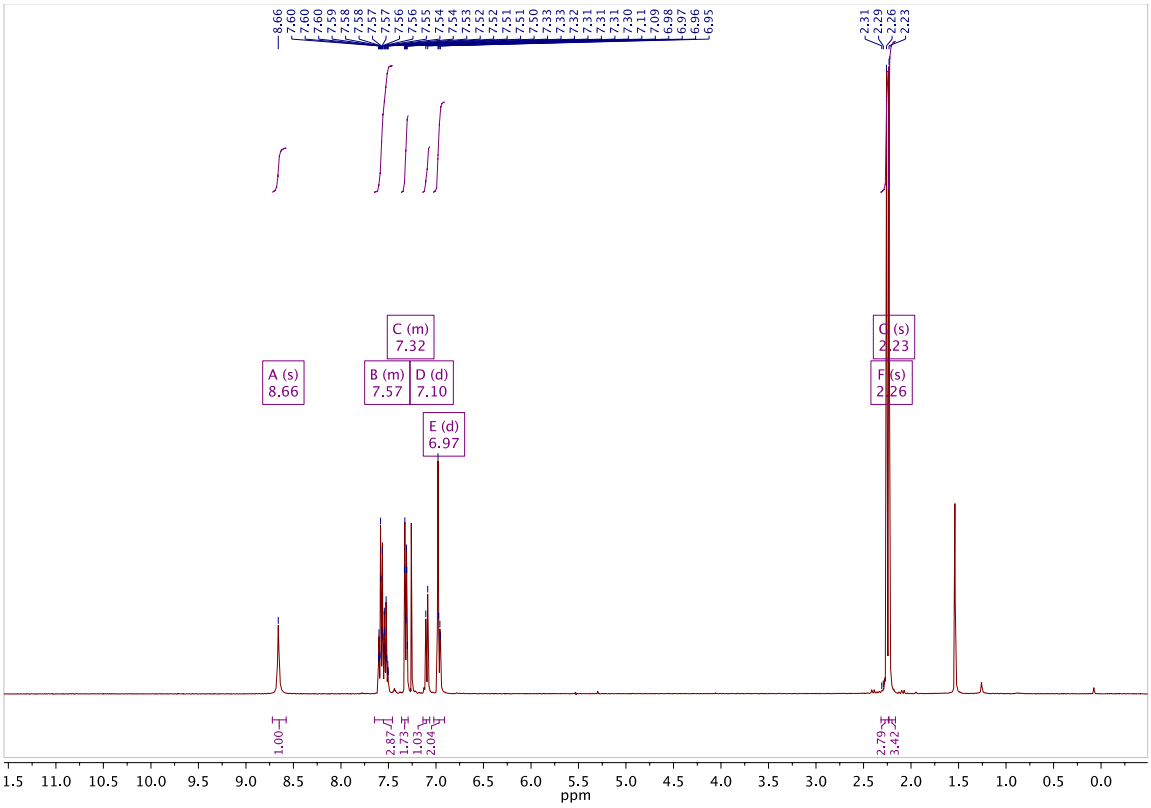

Fig. ESI20. 400.13 MHz ^{1}H NMR of (*E*) **-1b.**

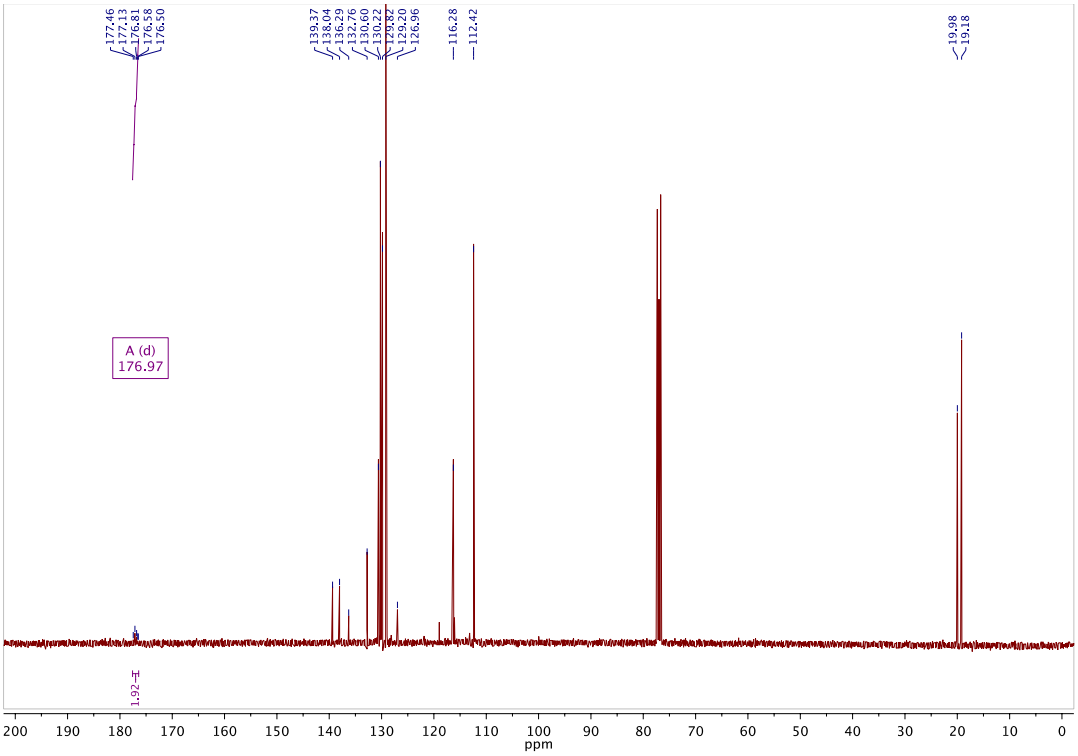

Figure ESI21. 100.62 MHZ ^{13}C NMR of (*E*)-**1b.**

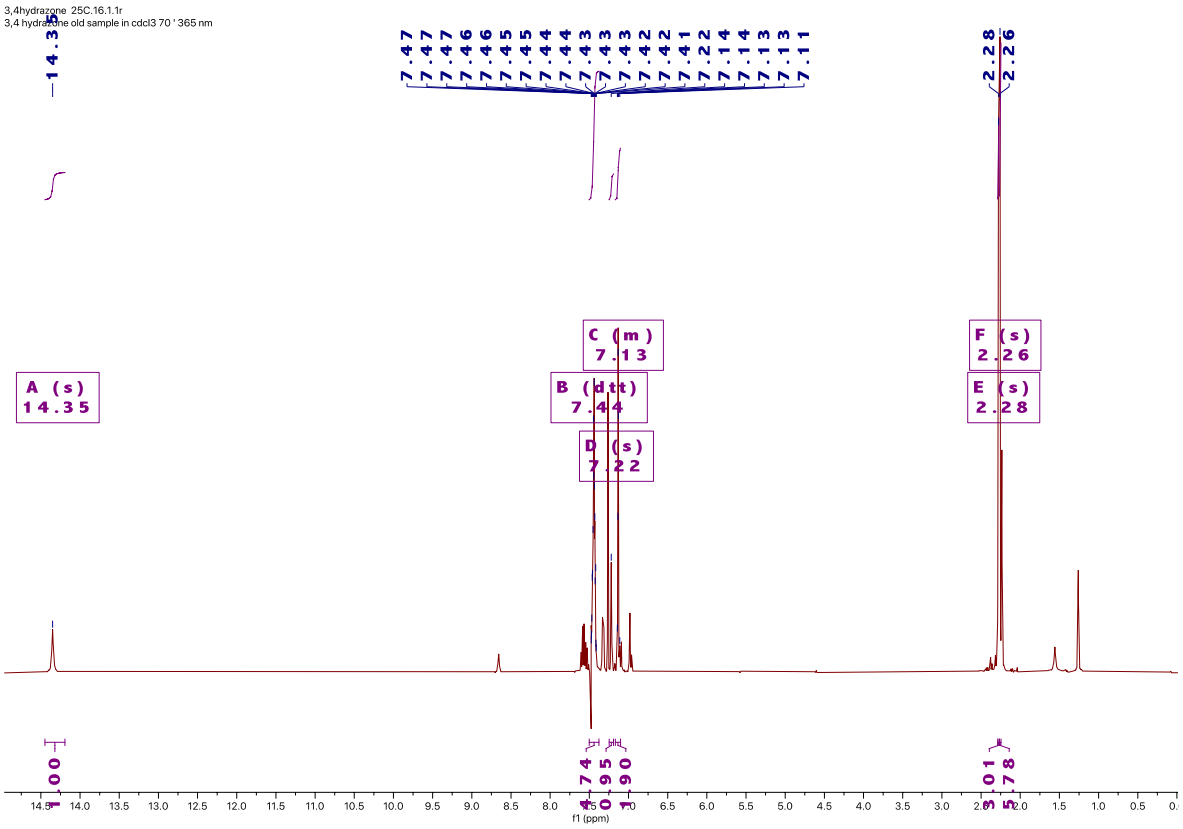

Fig. ESI22. 400.13 MHz ^{1}H NMR of (*Z*) **-1b.**

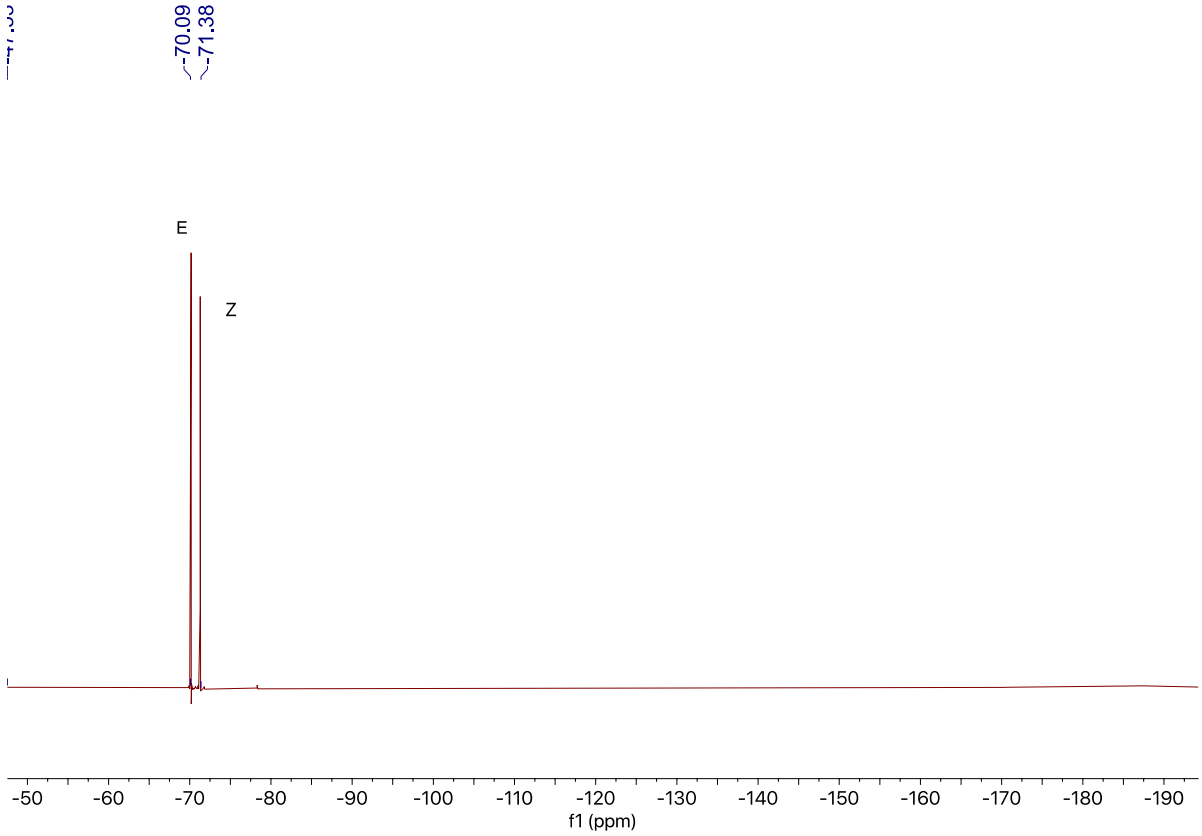

Fig. ESI23. 373.43 MHz ^{19}F NMR of **1b.**

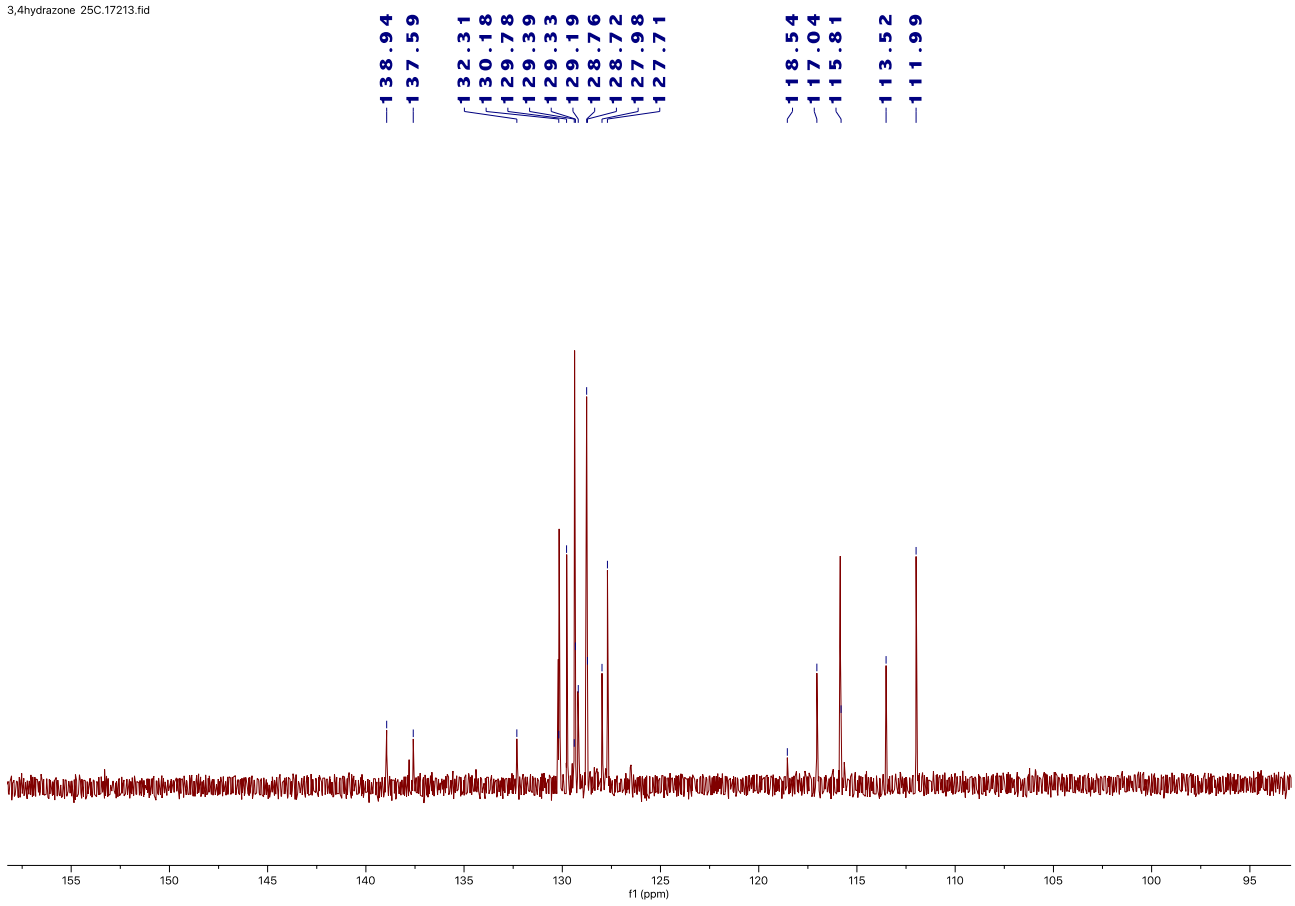

Fig. ESI24. 100.62 MHz ^{13}C NMR of **(*Z*)-1b.**

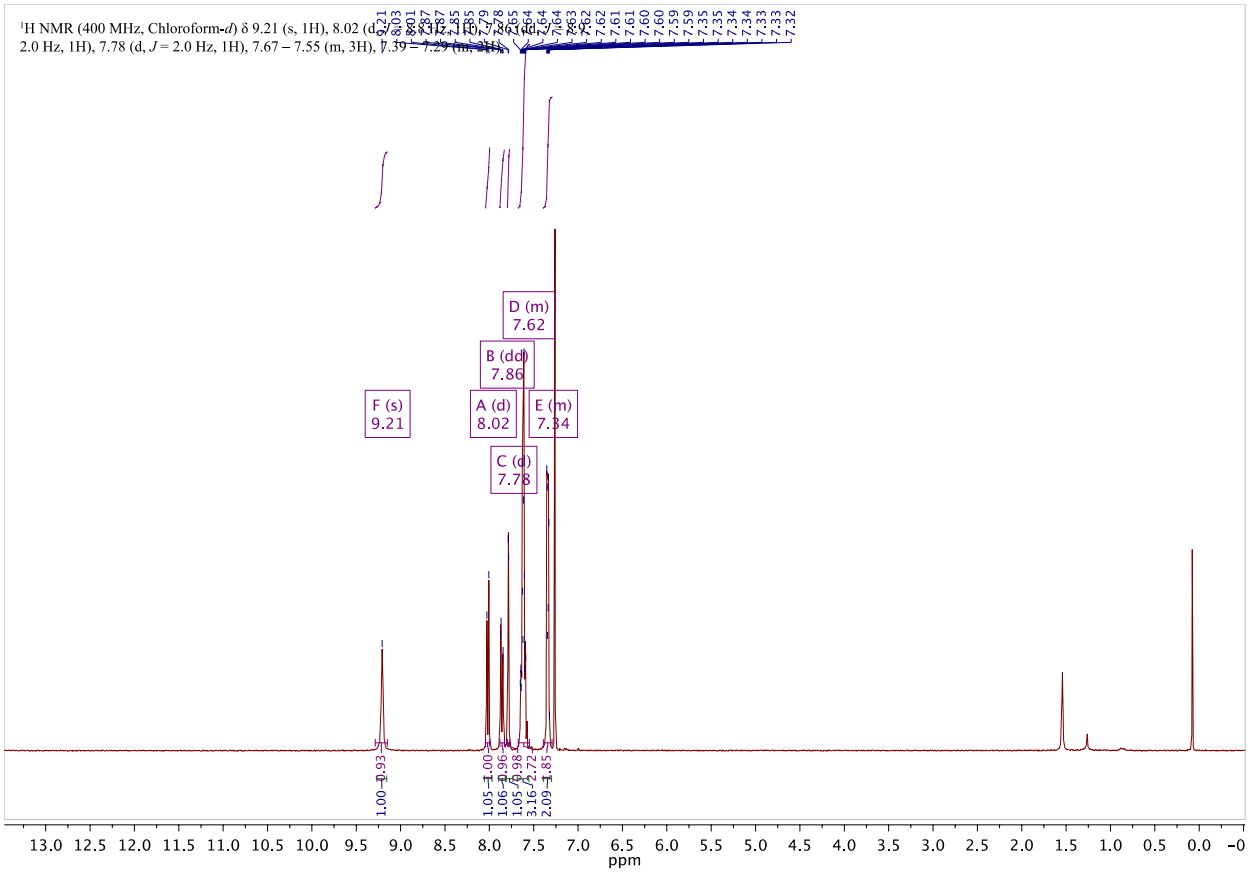

E

Fig. ESI25. 400.13 MHz ^{1}H NMR of **() -1c.**

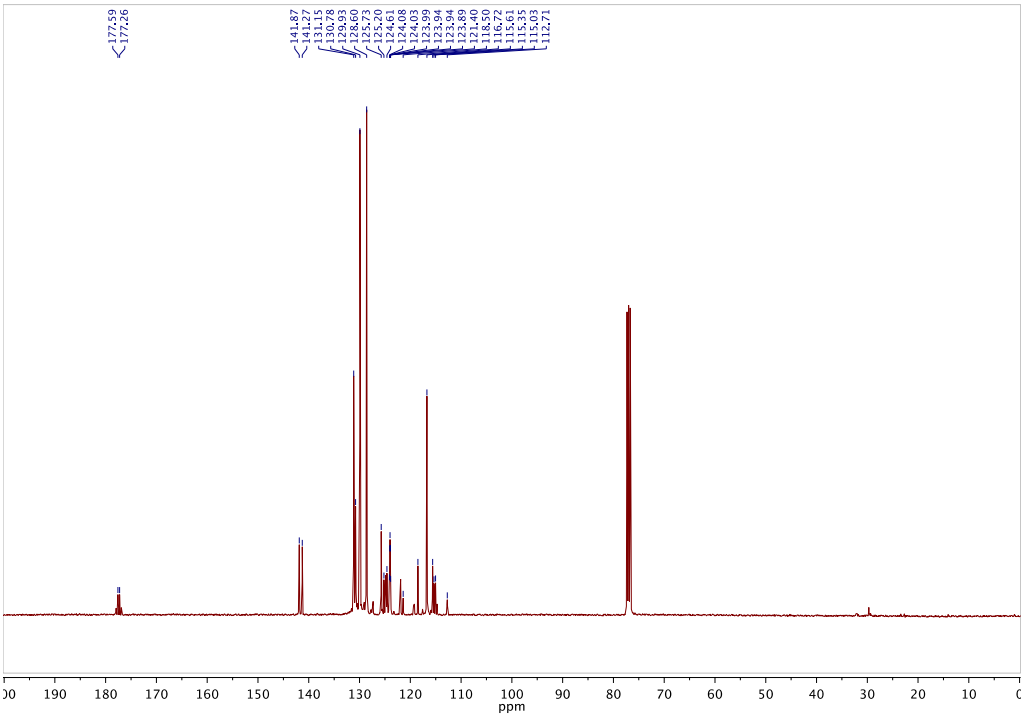

Fig ESI26. 100.62 MHz ^{13}C NMR of ***(E)*-1c**

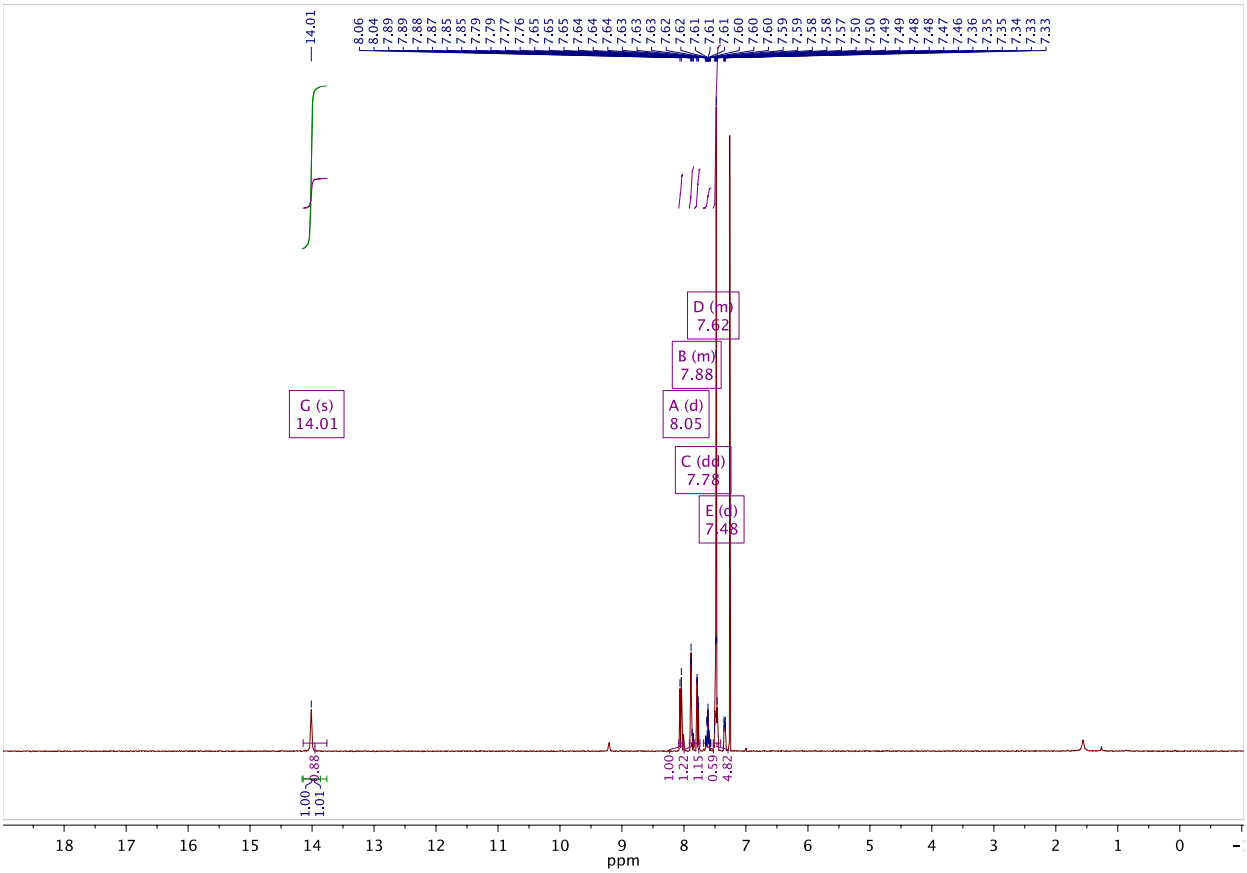

Fig. ESI27. 400.13 MHz ^{1}H NMR of (*Z)* **-1c.**

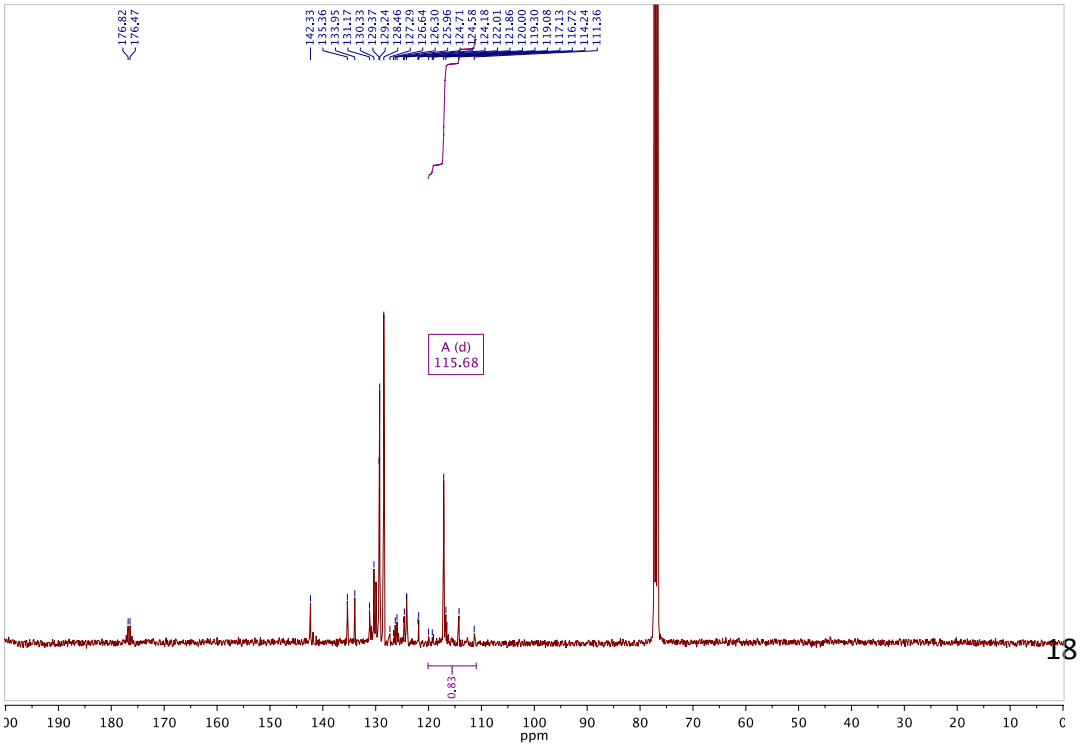

Fig. ESI28. 100.62 MHz ^{13}C NMR of (*Z*)**-1c.**

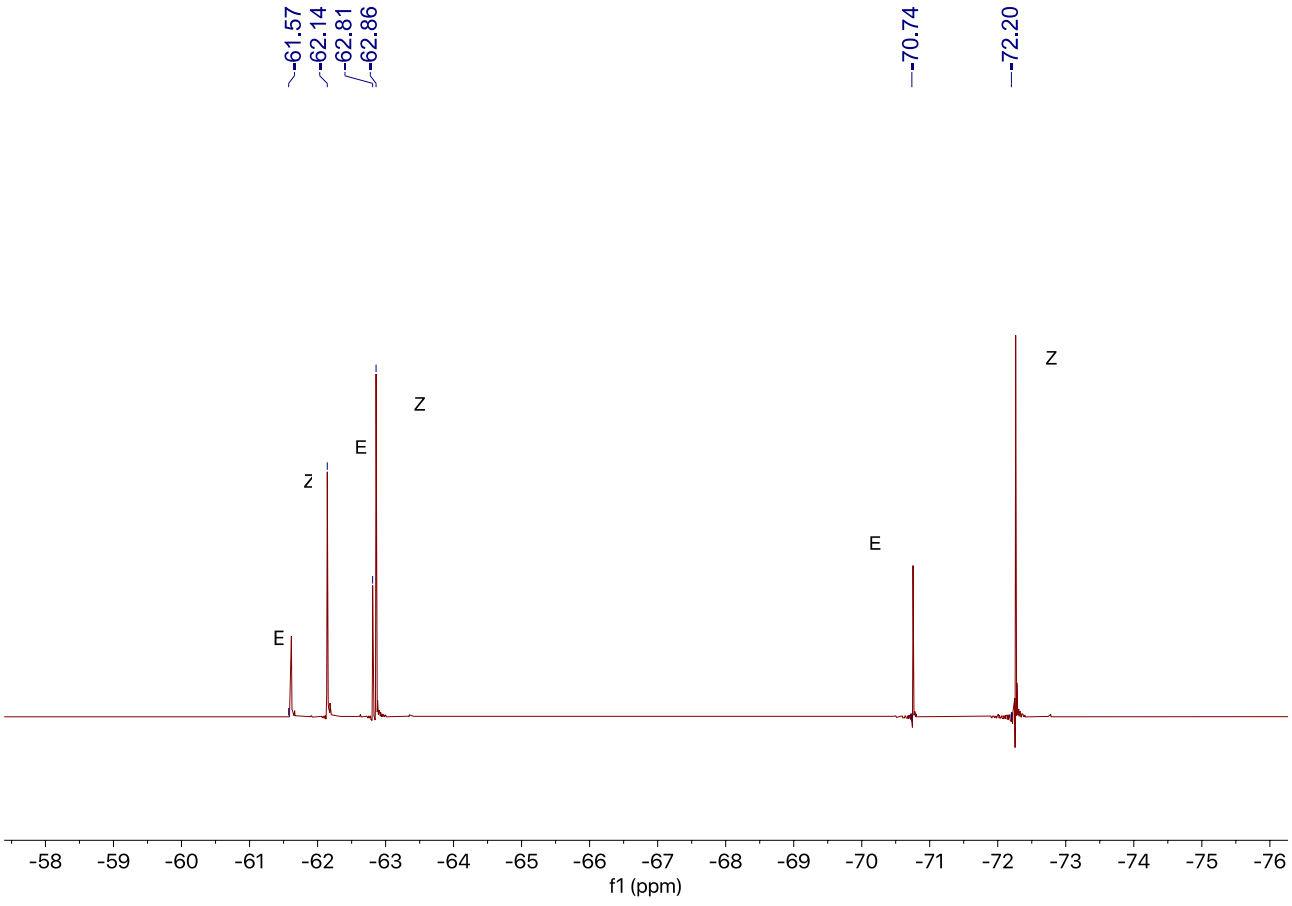

Fig. ESI29. 373.73 MHz ^{19}F NMR of (*E*)**-1c and** (*Z*)**-1c.**

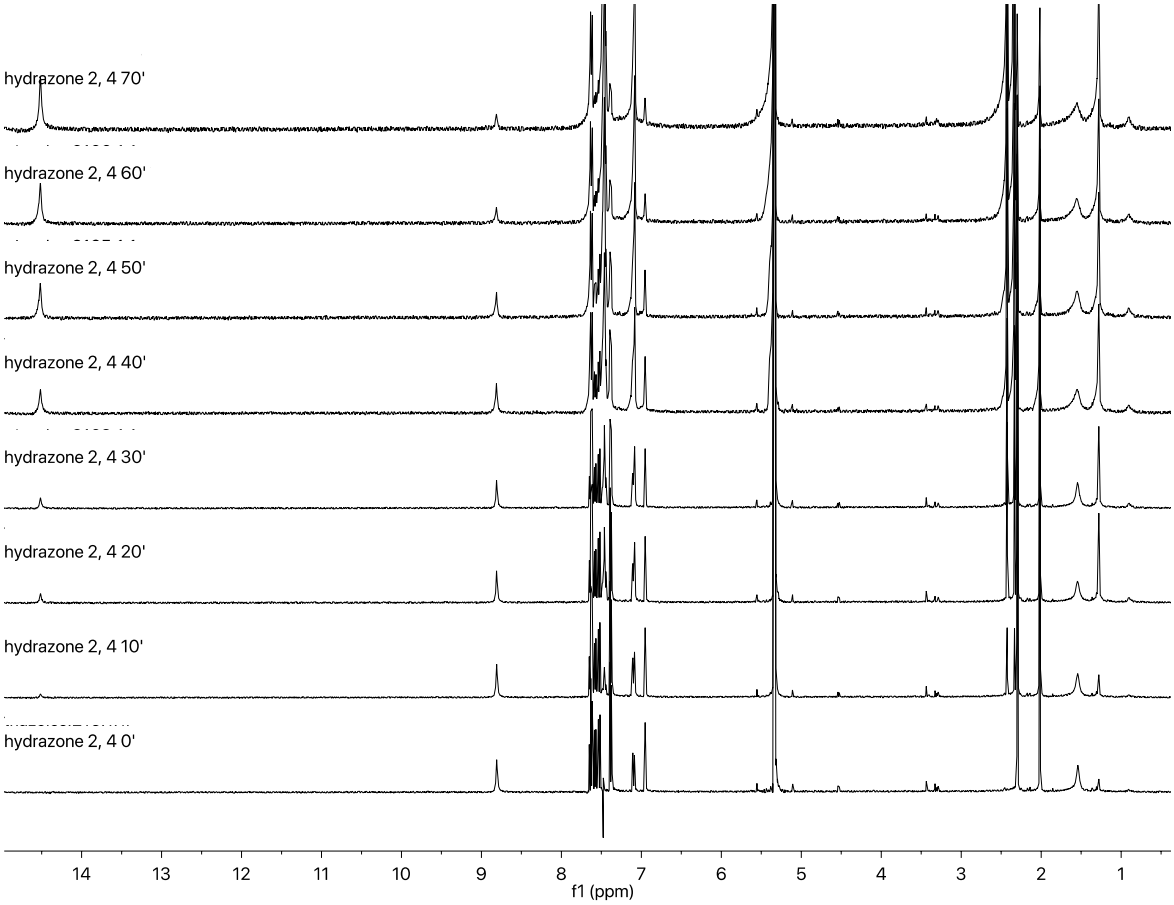

Fig. ESI30. NMR spectra in 1,1,2,2-tetrachloroethane-d_2 of (*E*)**-1a** irradiated at 365 nm time 0-70 min.

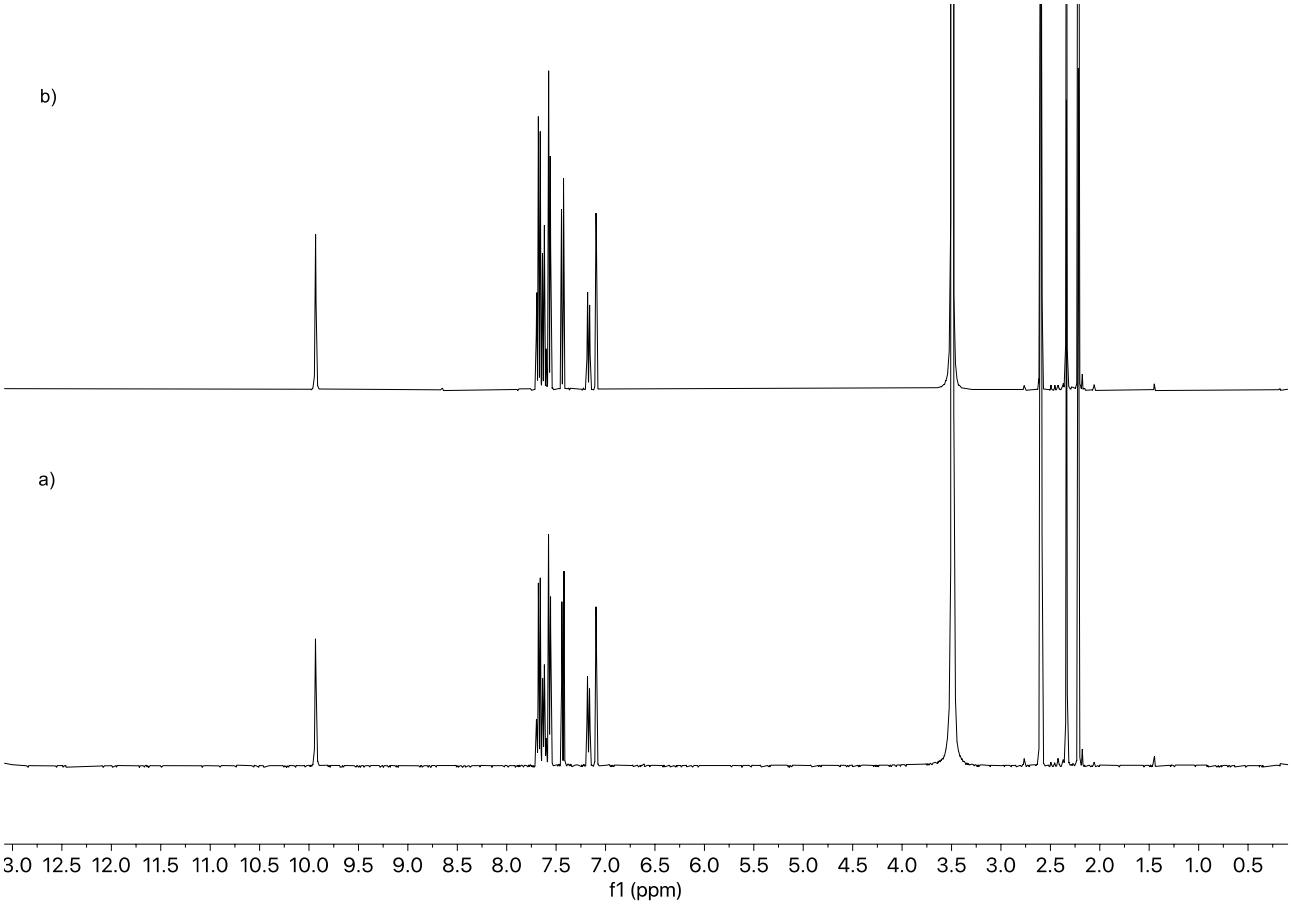

Fig. ESI31. NMR spectra in DMSO-d_6 of (*E*)**-1a a)** non irradiated **b)** irradiated at 365 nm 30 min.

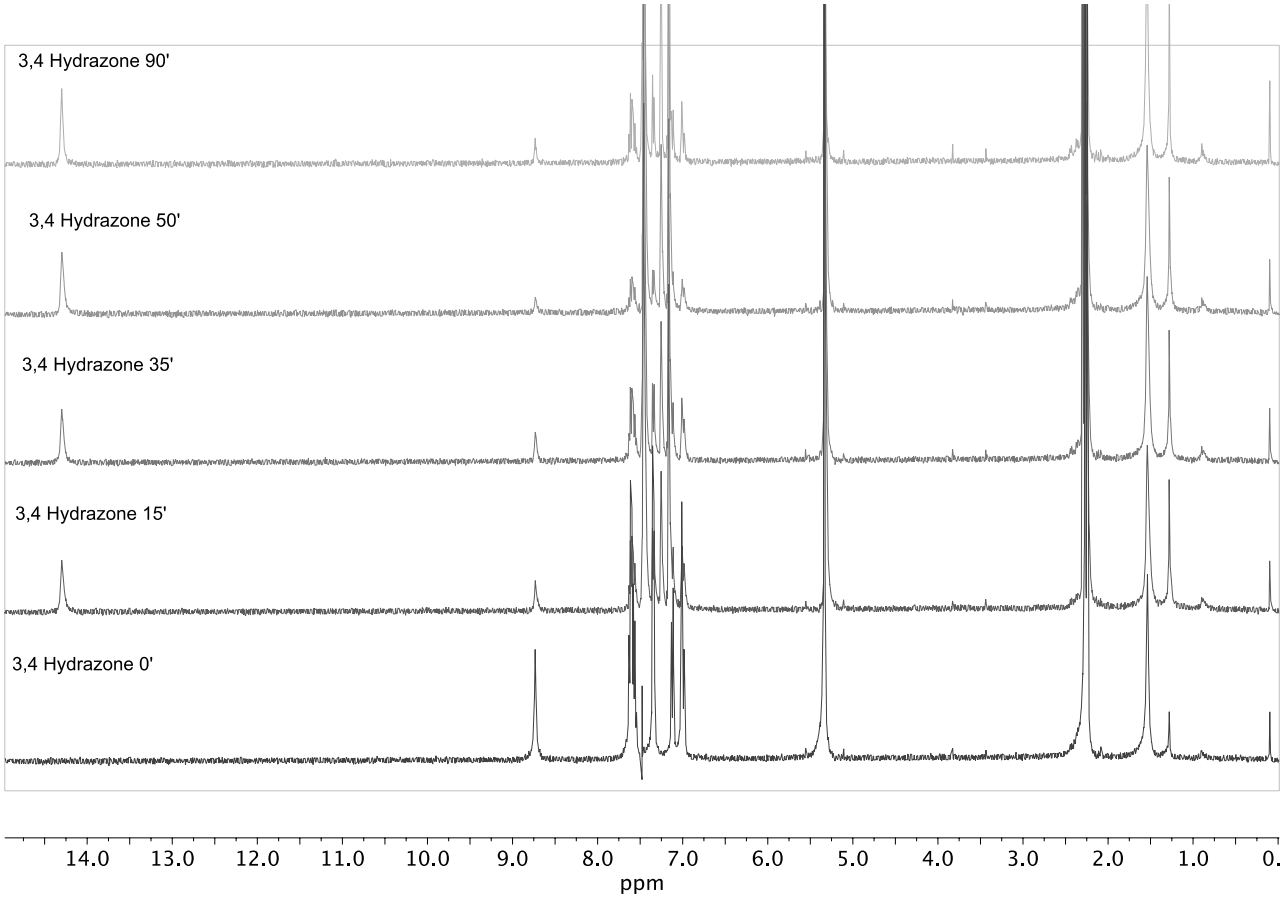

Fig. ESI32. NMR spectra in 1,1,2,2-tetrachloroethane-d_2 of (*E*)**-1b** irradiated at 365 nm time 0-90 min.

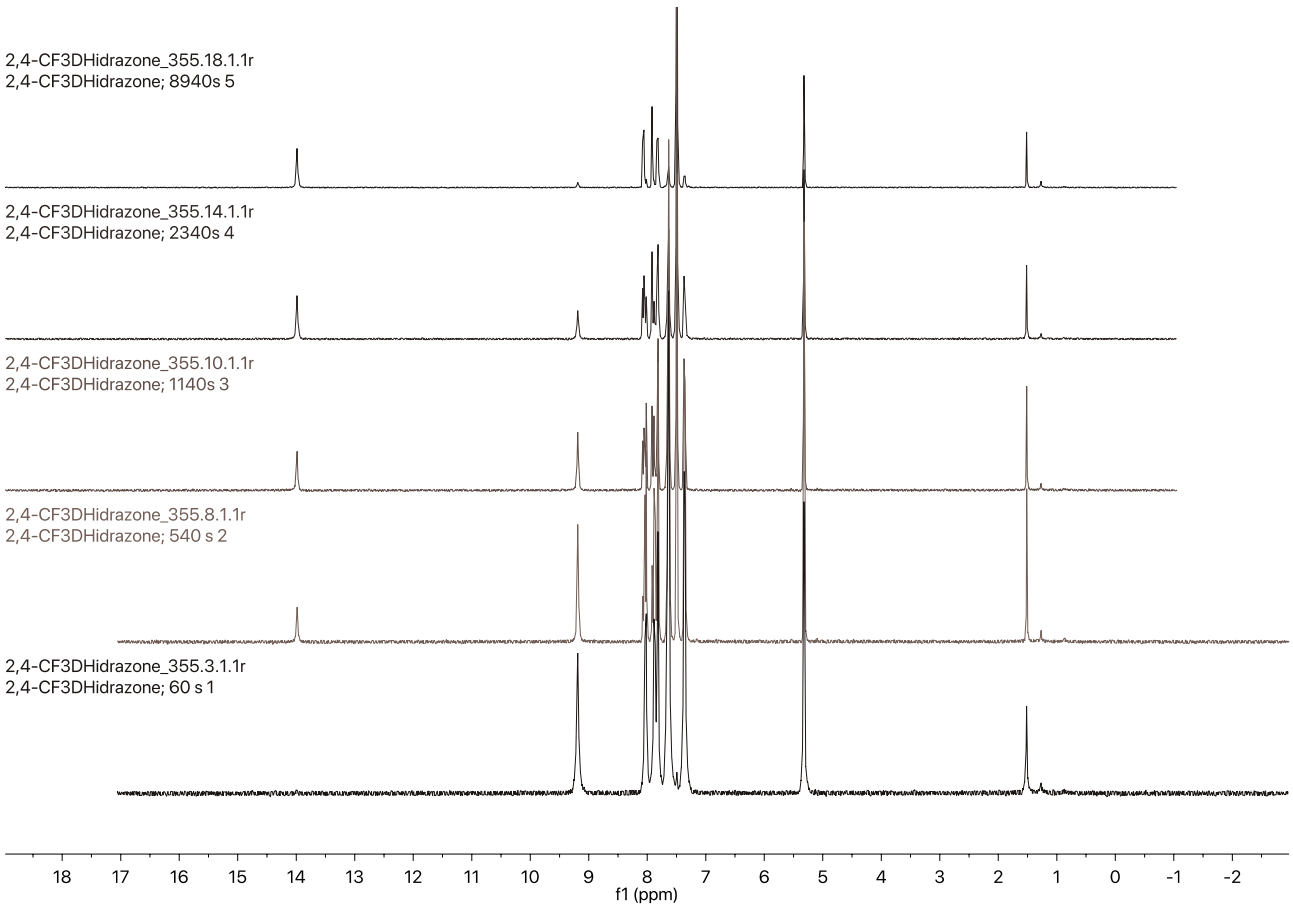

Fig. ESI33. NMR spectra in 1,1,2,2-tetrachloroethane-d_2 of **(*E*)-1c** irradiated at 365 nm time 0-70 min.

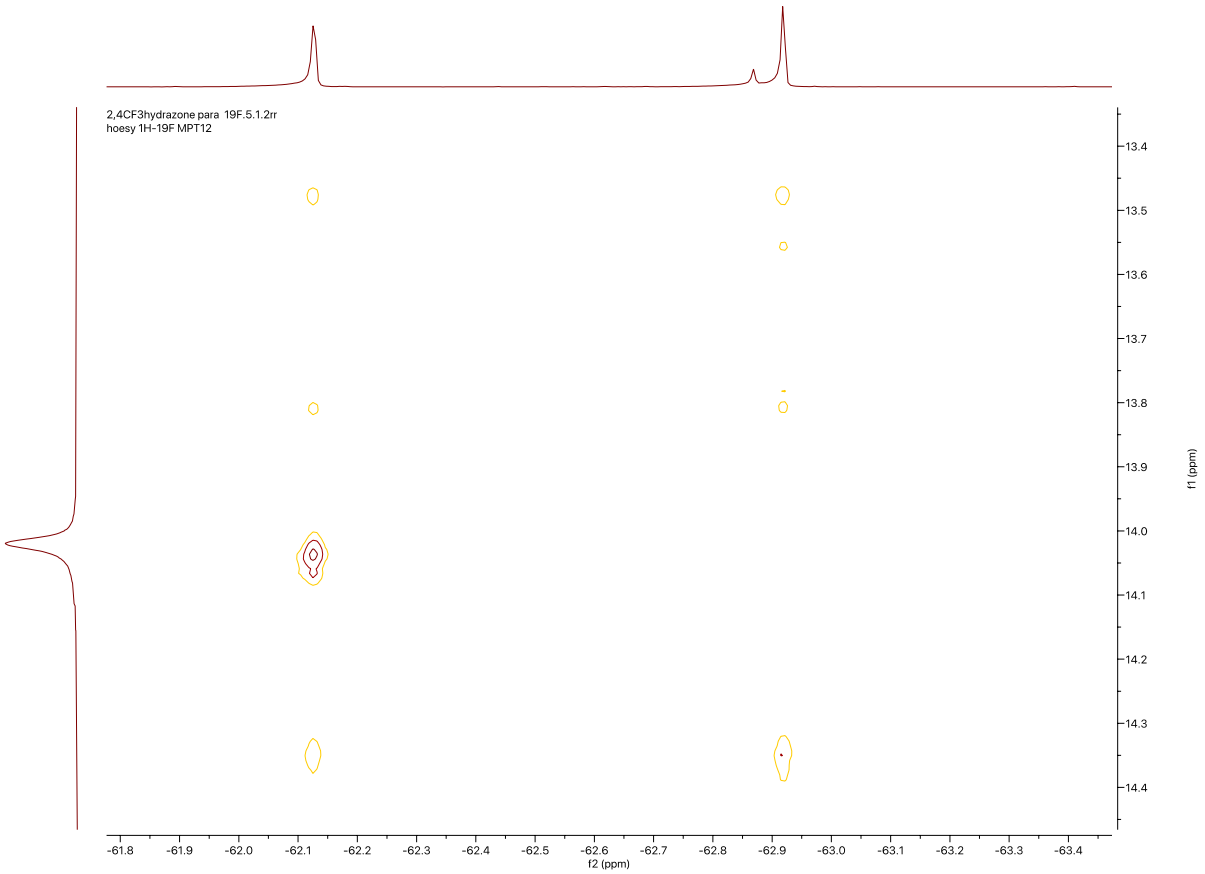

Fig. ESI34. ^{19}H-^{1}H HOESY experiment (d_8=550 ms) (*Z*)**-1c.**

3. X-Ray Analysis

(E)-1a

Crystal structure determination of *E*-1a

The asymmetric unit contains two crystallographically independent but chemically equivalent molecules, there are eight molecules in the unit cell.
The non-chiral molecule has crystallised in a chiral space group (this sometimes happens, there will be equal numbers of left and right handed crystals). The crystal chosen also had racemic twinning (there is a small twin component of the opposite handedness). The ratio of the two possible chiral domains in the crystal measured refined to 0.84:0.16 using the TWIN and BASF commands in Shelxl.
The NHs were located in a difference map but placed at a calculated position for the refinement.

Experimental

Single crystals of C17H15F3N2O were grown from methanol. A suitable crystal was selected and mounted on a glass fibre with Fomblin oil and placed on a Rigaku Oxford Diffraction SuperNova diffractometer with a duel source (Cu at zero) equipped with an AtlasS2 CCD area detector. The crystal was kept at 150(2) K during data collection. Using Olex2 [1], the structure was solved with the ShelXT [2] structure solution program using Intrinsic Phasing and refined with the ShelXL [3] refinement package using Least Squares minimisation.
Crystal Data for C17H15F3N2O (M =320.31 g/mol): orthorhombic, space group P212121 (no. 19), a = 8.14933(8) Å, b = 10.51816(9) Å, c = 36.3202(3) Å, V = 3113.22(5) Å3, Z = 8, T = 150(2) K, μ(CuKα) = 0.946 mm-1, Dcalc = 1.367 g/cm3, 30520 reflections measured (8.752° ≤ 2Θ ≤ 147.298°), 6180 unique (Rint = 0.0225, Rsigma = 0.0153) which were used in all calculations. The final R1 was 0.0267 (I > 2σ(I)) and wR2 was 0.0697 (all data).

Table 1 Crystal data and structure refinement for af9.

Identification code	af9
Empirical formula	$C_{17}H_{15}F_3N_2O$
Formula weight	320.31
Temperature/K	150(2)
Crystal system	orthorhombic
Space group	$P2_12_12_1$
a/Å	8.14933(8)
b/Å	10.51816(9)
c/Å	36.3202(3)
α/°	90
β/°	90
γ/°	90
Volume/Å^3	3113.22(5)
Z	8
ρ_{calc}g/cm^3	1.367

μ/mm^{-1}	0.946
F(000)	1328.0
Crystal size/mm^3	0.2 × 0.16 × 0.08 yellow block
Radiation	CuKα (λ = 1.54184)
2Θ range for data collection/°	8.752 to 147.298
Index ranges	-10 ≤ h ≤ 9, -13 ≤ k ≤ 13, -43 ≤ l ≤ 44
Reflections collected	30520
Independent reflections	6180 [R_{int} = 0.0225, R_{sigma} = 0.0153]
Data/restraints/parameters	6180/0/420
Goodness-of-fit on F^2	1.055
Final R indexes [I>=2σ (I)]	R_1 = 0.0267, wR_2 = 0.0688
Final R indexes [all data]	R_1 = 0.0278, wR_2 = 0.0697
Largest diff. peak/hole / e Å^{-3}	0.15/-0.20
Flack parameter	0.16(10)

Table 2 Fractional Atomic Coordinates (×10^4) and Equivalent Isotropic Displacement Parameters (Å^2×10^3) for af9. U_{eq} is defined as 1/3 of of the trace of the orthogonalised U_{IJ} tensor.

Atom	*x*	*y*	*z*	U(eq)
F1B	3512.5(13)	8721.9(10)	5996.8(3)	34.4(2)
F1E	8392.9(14)	8599.8(10)	6626.0(3)	37.5(2)
F1C	896.8(13)	9012.4(11)	6001.4(3)	39.7(3)
F1F	5825.5(14)	9051.7(12)	6594.0(3)	45.1(3)
F1A	2515.3(19)	10478.2(10)	6189.1(3)	48.5(3)
F1D	7619.1(19)	10431.3(10)	6435.9(4)	51.8(3)
O102	2244.3(18)	9517.3(12)	6834.0(3)	36.5(3)
O008	7409.5(19)	9524.4(12)	5779.7(4)	41.2(3)
N104	1911.5(17)	6731.8(13)	6337.1(4)	25.5(3)
N204	6661.0(18)	6698.9(13)	6240.6(4)	27.5(3)
N105	1698.4(19)	5490.0(13)	6332.5(4)	27.9(3)
N205	6329(2)	5471.7(13)	6196.0(4)	29.1(3)
C206	5677(2)	4748.7(15)	6487.6(4)	25.9(3)
C207	5236(2)	3486.2(15)	6414.9(5)	27.0(3)
C203	6995(2)	7378.1(16)	5950.5(4)	26.4(3)
C102	2147(2)	8735.2(16)	6592.3(5)	26.5(3)
C212	7023(2)	6877.4(16)	5567.1(4)	26.6(3)
C101	2278(2)	9227.9(16)	6189.2(5)	29.7(4)
C103	1851(2)	7374.3(15)	6644.9(4)	24.9(3)
C112	1465(2)	6869.1(15)	7016.0(5)	26.9(3)
C106	1781(2)	4834.6(16)	5993.6(5)	27.1(3)
C211	5447(2)	5277.8(16)	6834.7(5)	29.8(4)
C107	1069(2)	3624.4(16)	5970.3(5)	30.5(4)
C202	7233(2)	8733.8(16)	6018.7(5)	30.0(4)
C113	2366(2)	7247.1(18)	7324.4(5)	33.0(4)
C210	4709(2)	4561.9(17)	7109.3(5)	32.6(4)

C201	7264(2)	9198.0(17)	6424.0(5)	32.4(4)
C213	8095(2)	5895.3(17)	5476.6(5)	32.5(4)
C117	161(2)	6019.5(17)	7062.5(5)	31.2(4)
C217	5949(3)	7335.5(18)	5301.1(5)	35.3(4)
C209	4199(2)	3321.2(17)	7042.4(5)	32.6(4)
C208	4491(2)	2804.0(16)	6697.2(5)	31.6(4)
C111	2491(2)	5402.4(17)	5688.0(5)	31.4(4)
C108	1093(2)	3023.0(17)	5628.8(5)	35.2(4)
C110	2480(3)	4777.3(18)	5352.6(5)	35.6(4)
C114	1991(3)	6761(2)	7668.9(5)	41.2(4)
C116	-191(3)	5520.7(19)	7407.0(5)	38.0(4)
C109	1774(3)	3583.1(18)	5316.2(5)	37.5(4)
C214	8063(3)	5360.7(19)	5128.1(5)	38.4(4)
C27A	5524(2)	2896.9(16)	6040.8(5)	34.3(4)
C216	5924(3)	6793(2)	4953.9(5)	42.9(5)
C17A	255(3)	3020.1(18)	6299.6(5)	37.5(4)
C215	6963(3)	5795(2)	4869.2(5)	42.3(5)
C115	731(3)	5892(2)	7709.5(5)	42.6(5)
C29A	3312(3)	2575(2)	7336.4(6)	46.4(5)
C19A	1715(3)	2933(2)	4944.8(6)	51.6(6)

Table 3 Anisotropic Displacement Parameters ($Å^2×10^3$) for af9. The Anisotropic displacement factor exponent takes the form: $-2\pi^2[h^2a^{*2}U_{11}+2hka^*b^*U_{12}+\ldots]$.

Atom	U_{11}	U_{22}	U_{33}	U_{23}	U_{13}	U_{12}
F1B	28.5(5)	45.4(6)	29.4(5)	3.1(4)	6.5(4)	1.4(5)
F1E	33.7(6)	39.9(5)	39.0(6)	-0.8(4)	-9.9(4)	1.0(5)
F1C	28.7(5)	55.7(7)	34.6(5)	11.0(5)	-1.8(4)	3.0(5)
F1F	31.5(6)	58.2(7)	45.6(6)	-12.4(6)	1.5(5)	1.1(5)
F1A	72.3(9)	28.5(5)	44.6(6)	6.8(5)	7.4(6)	-3.5(6)
F1D	71.8(9)	27.3(5)	56.2(7)	-3.6(5)	-13.1(6)	-7.4(6)
O102	46.0(8)	31.1(6)	32.5(6)	-6.0(5)	6.9(6)	-1.9(6)
O008	47.9(8)	31.2(6)	44.4(7)	12.1(6)	-3.7(6)	-7.6(6)
N104	23.4(7)	24.8(6)	28.3(7)	0.4(5)	-0.4(5)	0.6(5)
N204	27.3(7)	25.7(6)	29.5(7)	2.4(5)	-1.7(6)	-2.9(6)
N105	31.8(8)	25.3(6)	26.5(7)	1.5(5)	-0.6(6)	0.2(6)
N205	37.9(8)	24.7(6)	24.7(7)	0.1(5)	1.7(6)	-4.9(6)
C206	25.2(8)	25.6(8)	27.0(8)	4.3(6)	-1.3(6)	-0.3(6)
C207	25.5(8)	24.0(7)	31.6(8)	1.8(6)	-4.8(7)	2.2(6)
C203	22.4(8)	27.8(8)	29.0(8)	3.6(6)	-0.5(6)	-0.9(6)
C102	23.1(8)	29.9(8)	26.7(8)	-1.1(6)	3.2(6)	1.4(6)
C212	22.3(8)	28.6(8)	29.1(8)	5.8(6)	1.2(6)	-2.8(7)
C101	28.9(9)	28.8(8)	31.3(8)	2.5(7)	3.2(7)	0.6(7)
C103	21.4(8)	27.7(8)	25.6(8)	1.2(6)	0.3(6)	1.0(6)
C112	25.3(8)	27.6(7)	27.8(8)	2.7(6)	2.8(6)	5.2(7)
C106	24.0(8)	27.3(7)	30.0(8)	-2.1(6)	-3.4(7)	2.7(6)
C211	35.5(9)	24.8(8)	29.1(8)	1.4(6)	-0.2(7)	-2.6(7)

C107	25.9(8)	26.9(8)	38.5(9)	2.1(7)	-5.4(7)	2.6(7)
C202	23.4(8)	29.0(8)	37.5(9)	3.6(7)	-2.5(7)	-2.9(6)
C113	28.1(9)	40.2(9)	30.8(9)	2.7(7)	-1.2(7)	1.3(8)
C210	35.4(9)	34.2(9)	28.3(8)	3.1(7)	1.1(7)	0.3(8)
C201	28.6(9)	27.7(8)	40.9(9)	-0.1(7)	-4.8(7)	-1.9(7)
C213	28.3(9)	35.9(9)	33.4(9)	5.1(7)	0.6(7)	3.6(7)
C117	27.0(9)	33.4(8)	33.2(9)	1.7(7)	4.1(7)	1.5(7)
C217	32.9(10)	38.0(9)	35.1(9)	9.6(8)	-0.5(7)	4.8(8)
C209	27.6(9)	33.2(9)	36.9(9)	12.6(8)	0.1(7)	-0.3(7)
C208	30.5(9)	23.9(8)	40.3(9)	5.4(7)	-5.6(7)	-2.3(7)
C111	32.5(9)	29.7(8)	31.9(9)	-1.1(7)	0.0(7)	0.7(7)
C108	34.2(10)	25.0(8)	46.4(10)	-4.9(7)	-9.5(8)	1.6(7)
C110	41.2(11)	35.2(9)	30.4(9)	-0.7(7)	1.9(7)	4.9(8)
C114	37.1(10)	57.6(12)	29.1(9)	5.3(8)	-2.6(8)	5.3(9)
C116	33.3(10)	38.5(9)	42.2(10)	8.1(8)	10.6(8)	1.4(8)
C109	41.3(11)	33.9(9)	37.3(10)	-8.7(7)	-5.8(8)	8.4(8)
C214	40.9(11)	36.7(9)	37.7(9)	1.2(8)	8.7(8)	5.0(8)
C27A	39.4(10)	27.9(8)	35.8(9)	-3.6(7)	-4.4(8)	1.4(8)
C216	46.2(11)	51.2(11)	31.3(10)	10.0(8)	-7.4(8)	3.1(10)
C17A	35.2(10)	31.1(9)	46.2(11)	3.8(8)	-1.4(8)	-3.7(8)
C215	54.6(13)	46.4(11)	25.8(8)	2.8(8)	4.1(8)	-4.1(10)
C115	42.2(11)	53.1(12)	32.6(9)	14.9(9)	7.2(8)	9.7(9)
C29A	44.6(12)	47.7(11)	47.0(11)	17.9(9)	4.3(9)	-7.3(10)
C19A	64.0(15)	46.0(11)	44.8(12)	-16.5(9)	-4.6(11)	9.3(11)

Table 4 Bond Lengths for af9.

Atom	Atom	Length/Å	Atom	Atom	Length/Å
F1B	C101	1.336(2)	C103	C112	1.483(2)
F1E	C201	1.335(2)	C112	C113	1.397(2)
F1C	C101	1.335(2)	C112	C117	1.399(2)
F1F	C201	1.334(2)	C106	C107	1.401(2)
F1A	C101	1.329(2)	C106	C111	1.387(2)
F1D	C201	1.330(2)	C211	C210	1.387(2)
O102	C102	1.206(2)	C107	C108	1.393(3)
O008	C202	1.211(2)	C107	C17A	1.508(3)
N104	N105	1.3178(19)	C202	C201	1.551(3)
N104	C103	1.307(2)	C113	C114	1.386(3)
N204	N205	1.329(2)	C210	C209	1.391(3)
N204	C203	1.302(2)	C213	C214	1.385(3)
N105	C106	1.412(2)	C117	C116	1.387(2)
N205	C206	1.408(2)	C217	C216	1.384(3)
C206	C207	1.401(2)	C209	C208	1.387(3)
C206	C211	1.391(2)	C209	C29A	1.510(3)
C207	C208	1.391(2)	C111	C110	1.384(2)
C207	C27A	1.512(2)	C108	C109	1.394(3)

C203 C212	1.489(2)	C110 C109	1.388(3)
C203 C202	1.460(2)	C114 C115	1.383(3)
C102 C101	1.557(2)	C116 C115	1.387(3)
C102 C103	1.464(2)	C109 C19A	1.513(3)
C212 C213	1.392(3)	C214 C215	1.378(3)
C212 C217	1.390(2)	C216 C215	1.383(3)

Table 5 Bond Angles for af9.

Atom Atom Atom	Angle/°	Atom Atom Atom	Angle/°
C103 N104 N105	121.23(14)	C210 C211 C206	119.55(16)
C203 N204 N205	118.47(14)	C106 C107 C17A	121.14(17)
N104 N105 C106	119.26(14)	C108 C107 C106	117.42(17)
N204 N205 C206	120.64(14)	C108 C107 C17A	121.41(16)
C207 C206 N205	117.84(15)	O008 C202 C203	124.40(17)
C211 C206 N205	121.11(15)	O008 C202 C201	117.53(16)
C211 C206 C207	121.04(15)	C203 C202 C201	118.07(15)
C206 C207 C27A	121.22(15)	C114 C113 C112	120.21(18)
C208 C207 C206	117.51(16)	C211 C210 C209	120.90(17)
C208 C207 C27A	121.25(15)	F1E C201 C202	112.62(15)
N204 C203 C212	124.48(15)	F1F C201 F1E	107.27(15)
N204 C203 C202	115.23(15)	F1F C201 C202	112.88(15)
C202 C203 C212	120.14(14)	F1D C201 F1E	106.96(15)
O102 C102 C101	116.94(15)	F1D C201 F1F	106.79(16)
O102 C102 C103	125.65(16)	F1D C201 C202	109.97(15)
C103 C102 C101	117.35(14)	C214 C213 C212	120.37(17)
C213 C212 C203	119.55(15)	C116 C117 C112	120.51(18)
C217 C212 C203	121.19(16)	C216 C217 C212	120.00(18)
C217 C212 C213	119.21(16)	C210 C209 C29A	120.48(18)
F1B C101 C102	114.25(14)	C208 C209 C210	118.32(16)
F1C C101 F1B	107.47(14)	C208 C209 C29A	121.18(18)
F1C C101 C102	111.49(14)	C209 C208 C207	122.60(16)
F1A C101 F1B	106.52(15)	C110 C111 C106	119.78(17)
F1A C101 F1C	106.90(15)	C107 C108 C109	122.62(17)
F1A C101 C102	109.85(14)	C111 C110 C109	121.11(18)
N104 C103 C102	112.80(14)	C115 C114 C113	120.26(19)
N104 C103 C112	126.89(15)	C117 C116 C115	119.75(19)
C102 C103 C112	120.26(14)	C108 C109 C19A	121.49(18)
C113 C112 C103	121.05(16)	C110 C109 C108	118.01(17)
C113 C112 C117	118.96(16)	C110 C109 C19A	120.48(19)
C117 C112 C103	119.97(16)	C215 C214 C213	120.07(18)
C107 C106 N105	118.44(16)	C215 C216 C217	120.40(18)
C111 C106 N105	120.46(15)	C214 C215 C216	119.91(18)
C111 C106 C107	121.04(16)	C114 C115 C116	120.25(17)

Table 6 Hydrogen Atom Coordinates (Å×10⁴) and Isotropic Displacement Parameters (Å²×10³) for af9.

Atom	*x*	*y*	*z*	U(eq)
H105	1506.92	5073.73	6538.2	33
H205	6518.39	5107.37	5982.04	35
H211	5792.05	6123.96	6883.35	36
H113	3237.92	7839.32	7297.9	40
H210	4550.92	4923.57	7346.31	39
H213	8851.85	5590.07	5654.75	39
H117	-488.9	5782.47	6856.48	37
H217	5232.51	8020.68	5357.57	42
H208	4168.39	1950.25	6651.74	38
H111	2984.48	6217.66	5708.82	38
H108	626.92	2198.32	5607.94	42
H110	2962.4	5172.49	5143.84	43
H114	2602.02	7025.87	7878	49
H116	-1060.52	4927.14	7435.7	46
H214	8801.58	4693.5	5067.63	46
H27A	4828.88	3319.78	5857.89	52
H27B	5251.33	1990.09	6049.93	52
H27C	6679.83	2998.87	5972.04	52
H216	5187.88	7108.29	4772.67	51
H17A	1063.35	2911.37	6496.89	56
H17B	-189.1	2188.55	6229.77	56
H17C	-638.14	3567.77	6386.16	56
H215	6918.15	5410.6	4632.76	51
H115	495.38	5547.44	7945.49	51
H29A	3685.36	2854.91	7579.79	70
H29B	3546.15	1667.51	7306.06	70
H29C	2127.6	2719.25	7314.39	70
H19A	2822.86	2666.73	4874.1	77
H19B	1283.68	3526.28	4760.46	77
H19C	998.53	2186.64	4959.31	77

Refinement model description

Number of restraints - 0, number of constraints - unknown.

Details:

```
1. Twinned data refinement
 Scales: 0.84(10)
 0.16(10)
2. Fixed Uiso
 At 1.2 times of:
  All C(H) groups, All N(H) groups
 At 1.5 times of:
  All C(H,H,H) groups
3.a Aromatic/amide H refined with riding coordinates:
 N105(H105), N205(H205), C211(H211), C113(H113), C210(H210), C213(H213),
 C117(H117), C217(H217), C208(H208), C111(H111), C108(H108), C110(H110),
 C114(H114), C116(H116), C214(H214), C216(H216), C215(H215), C115(H115)
3.b Idealised Me refined as rotating group:
```

C27A(H27A,H27B,H27C), C17A(H17A,H17B,H17C), C29A(H29A,H29B,H29C), C19A(H19A,
H19B,H19C)

This report has been created with Olex2, compiled on 2018.05.29 svn.r3508 for OlexSys. Please let us know if there are any errors or if you would like to have additional features.

E-1b

Experimental

Single crystals of $C_{17}H_{15}F_3N_2O$ **(*E*3,4)**were grown from methanol A suitable crystal was selected and mounted on a glass fibre with Fomblin oil and placed on a Rigaku Oxford Diffraction SuperNova diffractometer with a duel source (Cu at zero) equipped with an AtlasS2 CCD area detector. The crystal was kept at 150(2) K during data collection. Using Olex2 [1], the structure was solved with the ShelXT [2] structure solution program using Intrinsic Phasing and refined with the ShelXL [3] refinement package using Least Squares minimisation.

Crystal Data for $C_{17}H_{15}F_3N_2O$ (M =320.31 g/mol): monoclinic, space group $P2_1/c$ (no. 14), a = 12.5454(2) Å, b = 8.12670(15) Å, c = 15.8452(2) Å, β = 108.6141(17)°, V = 1530.96(5) Å^3, Z = 4, T = 150(2) K, μ(CuKα) = 0.962 mm^{-1}, *Dcalc* = 1.390 g/cm^3, 14916 reflections measured (7.436° ≤ 2Θ ≤ 147.612°), 3052 unique (R_{int} = 0.0196, R_{sigma} = 0.0137) which were used in all calculations. The final R_1 was 0.0387 (I > 2σ(I)) and wR_2 was 0.1042 (all data).

Table 1 Crystal data and structure refinement for 1b.

Identification code	1b
Empirical formula	$C_{17}H_{15}F_3N_2O$
Formula weight	320.31
Temperature/K	150(2)
Crystal system	monoclinic
Space group	$P2_1/c$
a/Å	12.5454(2)
b/Å	8.12670(15)
c/Å	15.8452(2)
α/°	90
β/°	108.6141(17)
γ/°	90
Volume/Å^3	1530.96(5)
Z	4
ρ_{calc}g/cm^3	1.390
μ/mm^{-1}	0.962
F(000)	664.0
Crystal size/mm^3	0.2 × 0.2 × 0.2 yellow block
Radiation	CuKα (λ = 1.54184)
2Θ range for data collection/°	7.436 to 147.612
Index ranges	-15 ≤ h ≤ 15, -8 ≤ k ≤ 10, -19 ≤ l ≤ 19
Reflections collected	14916
Independent reflections	3052 [R_{int} = 0.0196, R_{sigma} = 0.0137]
Data/restraints/parameters	3052/0/210
Goodness-of-fit on F^2	1.033
Final R indexes [I>=2σ (I)]	R_1 = 0.0387, wR_2 = 0.1018

Final R indexes [all data] $R_1 = 0.0407$, $wR_2 = 0.1042$
Largest diff. peak/hole / e Å^{-3} 0.30/-0.26

Table 2 Fractional Atomic Coordinates (×10^4) and Equivalent Isotropic Displacement Parameters (Å^2×10^3) for af10. U_{eq} is defined as 1/3 of of the trace of the orthogonalised U_{IJ} tensor.

Atom	*x*	*y*	*z*	U(eq)
F1A	2490.1(6)	6725.7(11)	8527.8(6)	35.0(2)
F1C	3317.9(7)	4567.1(11)	9208.9(6)	39.0(2)
O2	5251.3(7)	7103.2(11)	9002.4(5)	26.4(2)
F1B	3771.6(8)	6945.9(15)	9792.1(6)	53.1(3)
N5	3073.1(8)	3990.2(13)	6642.8(6)	22.8(2)
N4	3288.0(8)	4813.5(13)	7391.3(6)	21.4(2)
C3	4291.0(10)	5450.9(15)	7761.2(7)	20.8(3)
C12	5230.0(9)	5456.5(15)	7377.7(7)	20.4(3)
C6	1964.7(10)	3499.0(15)	6175.1(8)	22.2(3)
C17	5037.0(10)	6043.3(15)	6511.9(8)	23.9(3)
C2	4429.5(10)	6295.7(16)	8594.2(7)	21.8(3)
C13	6303.0(10)	4917.5(16)	7866.8(8)	24.9(3)
C11	1765.1(10)	2790.5(16)	5340.6(8)	24.3(3)
C10	677.8(10)	2370.7(16)	4817.0(8)	25.4(3)
C7	1084.5(11)	3778.1(17)	6510.1(8)	27.6(3)
C14	7165.8(11)	4970.9(17)	7496.5(9)	29.5(3)
C16	5901.6(11)	6083.0(17)	6141.7(8)	27.9(3)
C9	-221.5(10)	2668.3(17)	5142.8(8)	27.0(3)
C15	6965.8(11)	5549.8(17)	6636.3(9)	29.5(3)
C1	3478.8(11)	6129.2(17)	9025.7(8)	27.6(3)
C8	4.5(11)	3352.6(18)	5986.7(9)	30.1(3)
C9A	-1413.7(11)	2256(2)	4593.0(10)	35.6(3)
C10A	476.2(12)	1643(2)	3903.8(9)	35.4(3)

Table 3 Anisotropic Displacement Parameters (Å^2×10^3) for af10. The Anisotropic displacement factor exponent takes the form: $-2\pi^2[h^2a^{*2}U_{11}+2hka^*b^*U_{12}+\ldots]$.

Atom	U_{11}	U_{22}	U_{33}	U_{23}	U_{13}	U_{12}
F1A	26.5(4)	39.3(5)	42.2(5)	-1.6(4)	15.1(3)	3.6(3)
F1C	41.3(5)	40.7(5)	41.5(5)	11.9(4)	22.2(4)	-2.3(4)
O2	23.9(4)	33.2(5)	21.2(4)	-4.6(4)	5.7(3)	-6.9(4)
F1B	41.9(5)	88.6(8)	36.9(5)	-35.1(5)	24.0(4)	-27.1(5)
N5	17.7(5)	28.8(6)	21.1(5)	-5.3(4)	5.2(4)	-0.8(4)
N4	21.0(5)	22.7(5)	18.8(5)	-0.9(4)	4.2(4)	-0.1(4)
C3	20.0(5)	22.5(6)	18.7(5)	1.0(4)	4.3(4)	-0.1(4)
C12	20.8(6)	20.6(6)	19.2(5)	-1.6(4)	5.5(4)	-1.9(4)
C6	18.5(5)	23.7(6)	22.5(6)	-0.4(5)	3.8(4)	-1.3(5)
C17	23.6(6)	25.2(6)	21.2(6)	2.4(5)	4.7(5)	0.8(5)
C2	20.7(5)	25.3(6)	19.0(5)	1.0(5)	5.5(4)	-1.5(5)
C13	24.0(6)	27.6(6)	21.0(6)	2.6(5)	4.4(5)	1.0(5)

C11	21.1(6)	27.3(6)	24.2(6)	-2.5(5)	6.9(5)	0.6(5)
C10	24.3(6)	25.4(6)	23.7(6)	-1.9(5)	3.8(5)	-1.3(5)
C7	24.1(6)	35.6(7)	23.3(6)	-5.1(5)	7.9(5)	-3.2(5)
C14	21.6(6)	33.2(7)	32.5(7)	2.7(5)	6.8(5)	4.2(5)
C16	32.7(6)	29.7(7)	23.1(6)	2.9(5)	11.4(5)	-1.2(5)
C9	20.9(6)	29.1(7)	28.5(6)	1.3(5)	4.3(5)	-3.8(5)
C15	28.9(6)	30.8(7)	33.9(7)	0.5(5)	17.1(5)	-0.7(5)
C1	25.8(6)	34.7(7)	23.1(6)	-6.6(5)	9.0(5)	-6.7(5)
C8	21.4(6)	38.8(8)	32.2(7)	-2.4(6)	11.3(5)	-3.2(5)
C9A	22.9(6)	44.7(8)	35.5(7)	-2.0(6)	4.1(5)	-8.0(6)
C10A	29.3(7)	43.9(8)	28.4(7)	-10.2(6)	2.7(5)	-1.2(6)

Table 4 Bond Lengths for af10.

Atom	Atom	Length/Å	Atom	Atom	Length/Å
F1A	C1	1.3308(15)	C6	C7	1.3880(17)
F1C	C1	1.3319(17)	C17	C16	1.3884(17)
O2	C2	1.2191(15)	C2	C1	1.5585(16)
F1B	C1	1.3286(15)	C13	C14	1.3869(18)
N5	N4	1.3127(14)	C11	C10	1.3939(17)
N5	C6	1.4086(15)	C10	C9	1.4035(18)
N4	C3	1.3131(15)	C10	C10A	1.5077(18)
C3	C12	1.4879(16)	C7	C8	1.3877(18)
C3	C2	1.4482(16)	C14	C15	1.3870(19)
C12	C17	1.3986(16)	C16	C15	1.3844(19)
C12	C13	1.3923(17)	C9	C8	1.3912(19)
C6	C11	1.3897(17)	C9	C9A	1.5088(17)

Table 5 Bond Angles for af10.

Atom	Atom	Atom	Angle/°	Atom	Atom	Atom	Angle/°
N4	N5	C6	120.22(10)	C11	C10	C9	119.19(11)
N5	N4	C3	119.70(10)	C11	C10	C10A	119.99(11)
N4	C3	C12	126.14(10)	C9	C10	C10A	120.81(11)
N4	C3	C2	114.39(10)	C8	C7	C6	118.36(11)
C2	C3	C12	119.37(10)	C13	C14	C15	120.37(12)
C17	C12	C3	119.34(10)	C15	C16	C17	119.73(11)
C13	C12	C3	121.51(10)	C10	C9	C9A	120.96(12)
C13	C12	C17	119.15(11)	C8	C9	C10	118.77(11)
C11	C6	N5	117.76(11)	C8	C9	C9A	120.27(12)
C7	C6	N5	121.65(11)	C16	C15	C14	120.11(12)
C7	C6	C11	120.52(11)	F1A	C1	F1C	107.40(10)
C16	C17	C12	120.56(11)	F1A	C1	C2	114.03(10)
O2	C2	C3	125.02(11)	F1C	C1	C2	111.64(11)
O2	C2	C1	116.74(10)	F1B	C1	F1A	107.06(11)
C3	C2	C1	118.21(10)	F1B	C1	F1C	107.09(11)

C14	C13	C12	120.08(11)	F1B	C1	C2	109.30(10)
C6	C11	C10	120.84(11)	C7	C8	C9	122.31(12)

Table 6 Hydrogen Bonds for af10.

D	H	A	d(D-H)/Å	d(H-A)/Å	d(D-A)/Å	D-H-A/°
N5	H5	O2[1]	0.88	2.21	3.0311(13)	155.9

[1]1-X,-1/2+Y,3/2-Z

Table 7 Hydrogen Atom Coordinates (Å×10⁴) and Isotropic Displacement Parameters (Å²×10³) for af10.

Atom	*x*	*y*	*z*	U(eq)
H5	3623.33	3744.39	6432.36	27
H17	4308.29	6417.9	6174.29	29
H13	6444.21	4512.68	8454.85	30
H11	2377.55	2589.72	5124.32	29
H7	1218.11	4248.82	7083.39	33
H14	7897.96	4609.02	7833.9	35
H16	5763.36	6474.37	5551.39	33
H15	7560.18	5580.53	6386.03	35
H8	-601.83	3534.98	6212.58	36
H9AA	-1583.69	2755.67	4001.64	53
H9AB	-1933.49	2686.81	4887.88	53
H9AC	-1498.42	1059.4	4532.19	53
H10A	-19.2	2371.54	3454.74	53
H10B	121.2	561.21	3873.46	53
H10C	1195.43	1524.65	3789.68	53

Refinement model description

Number of restraints - 0, number of constraints - unknown.

Details:

```
1. Fixed Uiso
 At 1.2 times of:
  All C(H) groups, All N(H) groups
 At 1.5 times of:
  All C(H,H,H) groups
2.a Aromatic/amide H refined with riding coordinates:
 N5(H5), C17(H17), C13(H13), C11(H11), C7(H7), C14(H14), C16(H16),
C15(H15),
 C8(H8)
2.b Idealised Me refined as rotating group:
 C9A(H9AA,H9AB,H9AC), C10A(H10A,H10B,H10C)
```

This report has been created with Olex2, compiled on 2018.05.29 svn.r3508 for OlexSys. Please let us know if there are any errors or if you would like to have additional features.

4. DFT calculations

Geometry optimizations have been carried out considering different starting points, corresponding to the different rotamers with respect to the bonds in the CO-C=N-NH-Ph segment (4 torsions involved). In all cases, both cis and trans isomers show only one clearly preferred conformation, the other ones being at least 5 kcal/mol less stable.

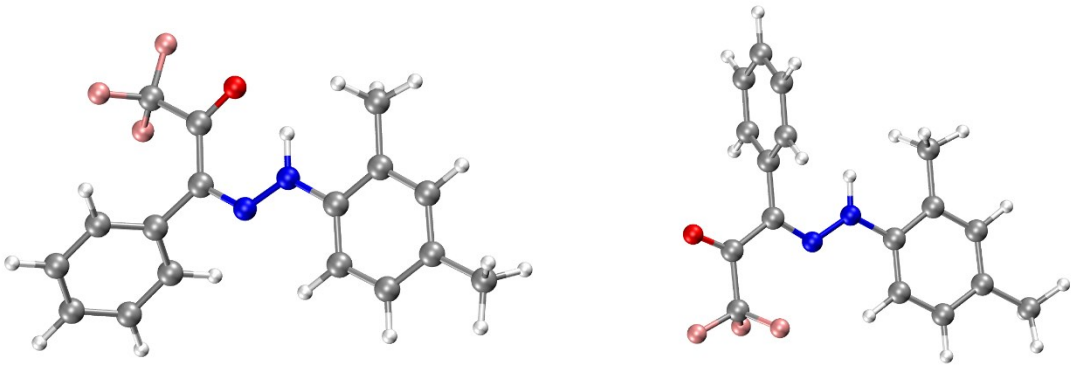

Fig. ESI35. Most stable minima for the *Z* and *E* isomers of hydrazone **1a**.

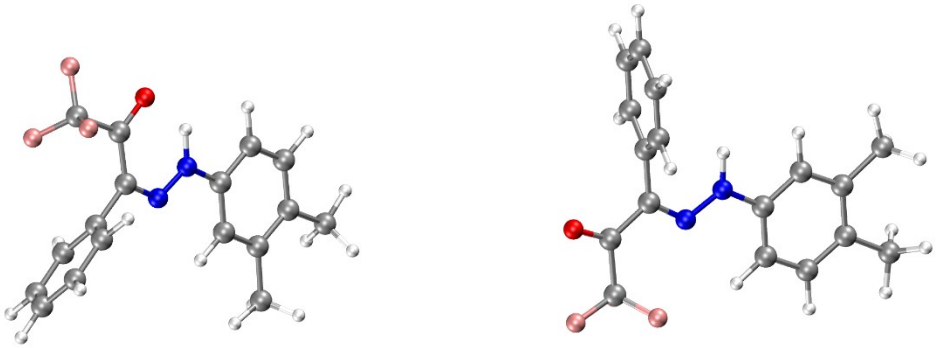

Fig. ESI36. Most stable minima for the cis and trans isomers of hydrazone **1b**.

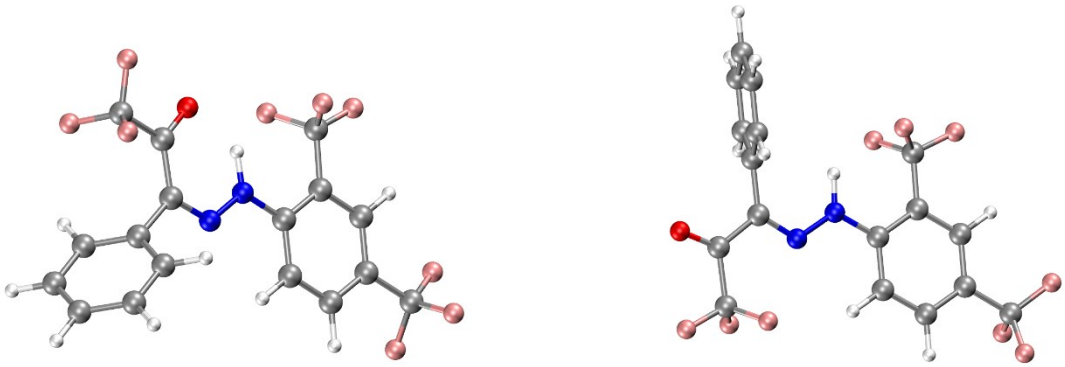

Fig. ESI37. EMost stable minima for the cis and trans isomers of hydrazone **1c.**

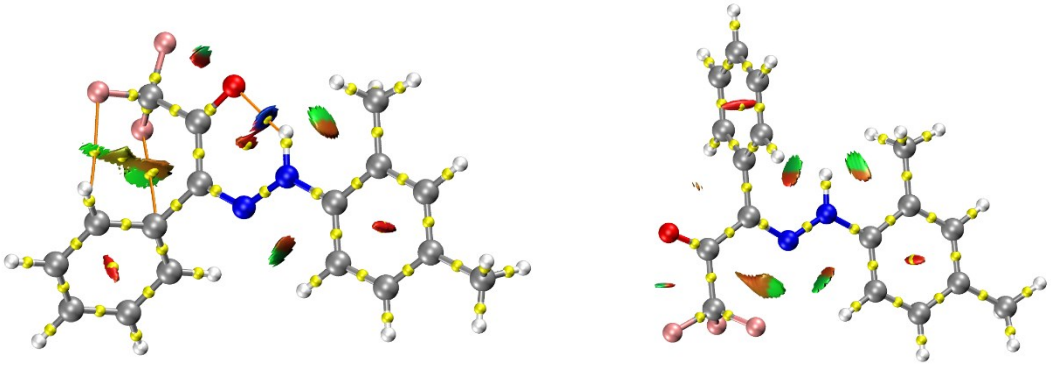

Fig. ESI38. Intramolecular non covalent interactions for the *Z* (left) and *E* (right*)* isomers of hydrazone **1a.**

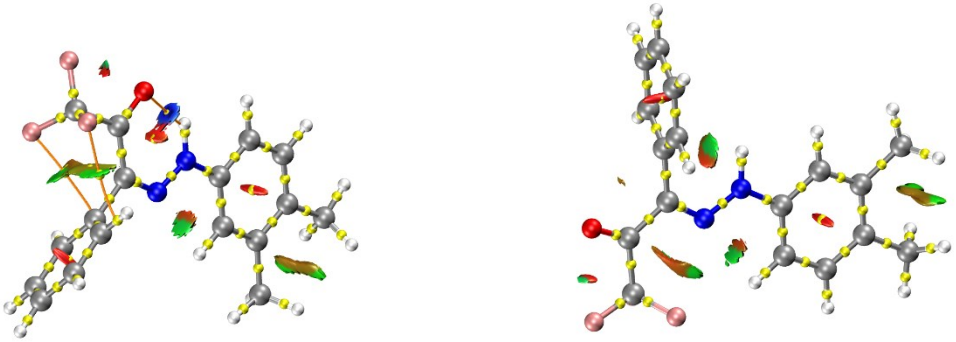

Fig. ESI39. Intramolecular non covalent interactions for the *Z*(left) and *E*(right) isomers of hydrazone **1b.**

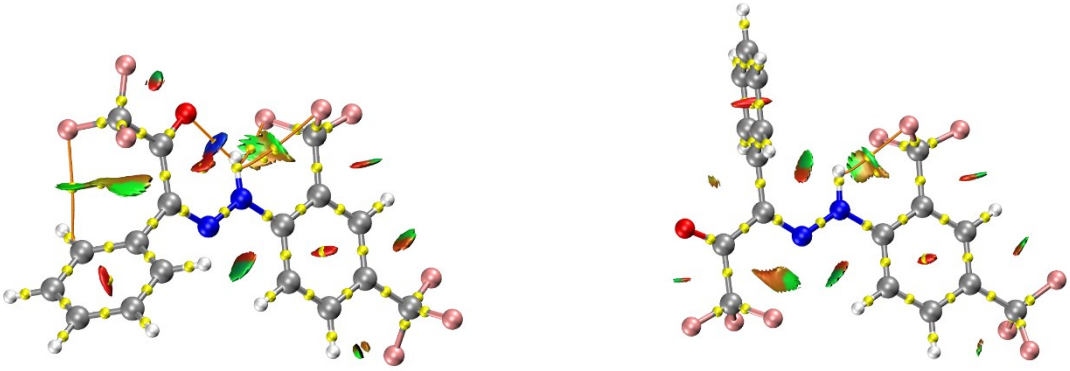

Fig. ESI40. Intramolecular non-covalent interactions for the *Z*(left) and *E* (right) isomers of hydrazone **1c**.

Absorption spectra

Excitation energies in the relevant geometries, have been analyzed by TD-DFT calculations, with inclusion of solvent effects.

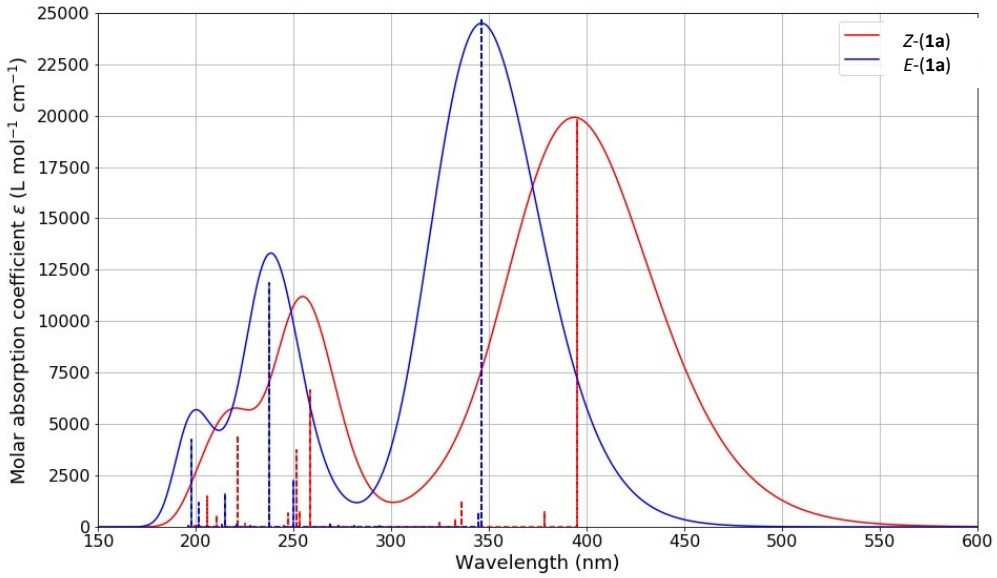

Fig. ESI41. Simulated absorption spectra for the *E* (blue) and *Z* (red) of hydrazone **1a** in the gas phase.

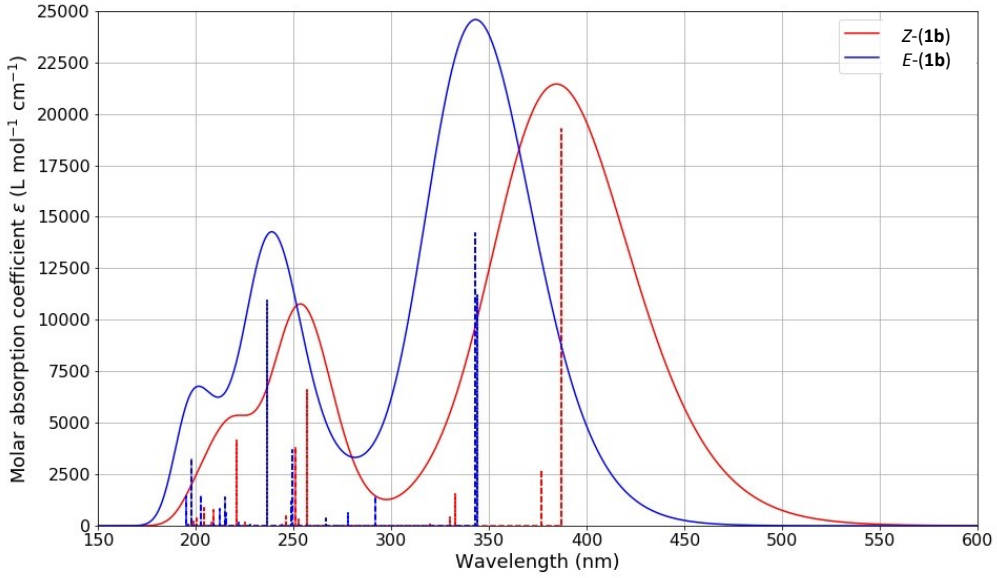

Fig. ESI42. Simulated absorption spectra for the *E* (blue) and *Z* (red) of hydrazone **1b** in the gas phase.

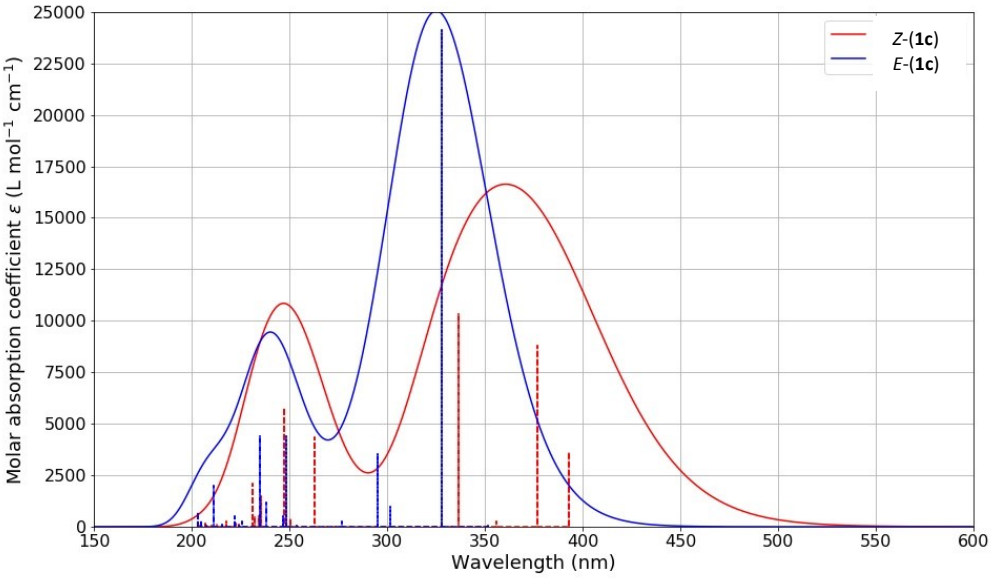

Fig. ESI43. Simulated absorption spectra for the *E* (blue) and *Z* (red) of hydrazone **1c** in the gas phase.

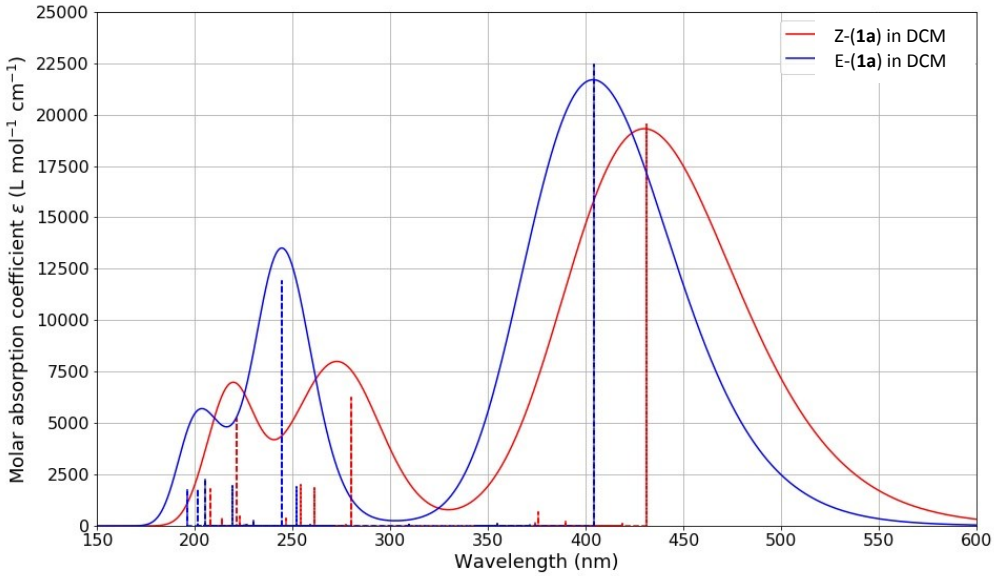

Fig. ESI44. Simulated absorption spectra for the *E* (blue) and *Z* (red) of hydrazone **1a** in dichloromethane

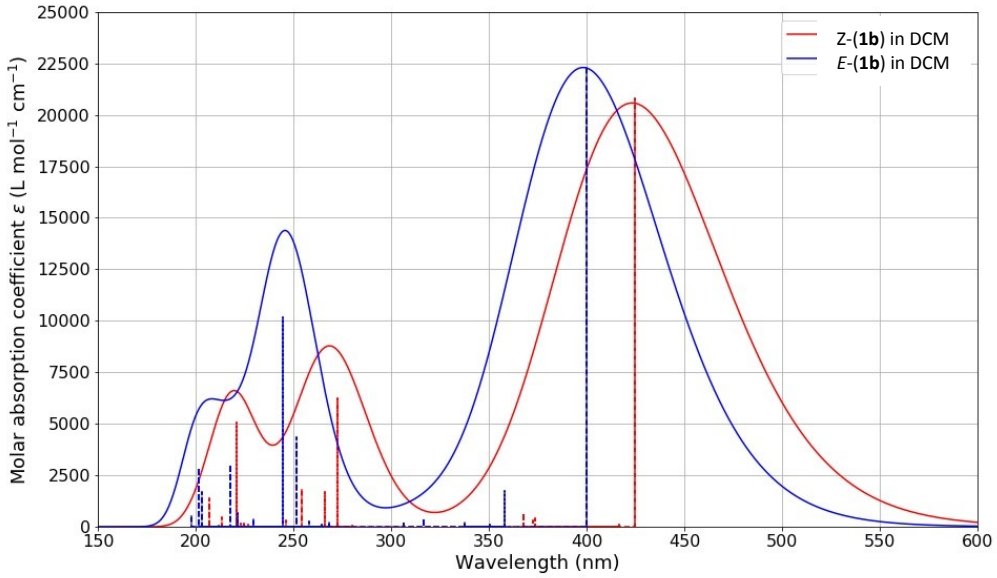

Fig. ESI45. Simulated absorption spectra for the *E* (blue) and *Z* (red) of hydrazone **1b** in dichloromethane.

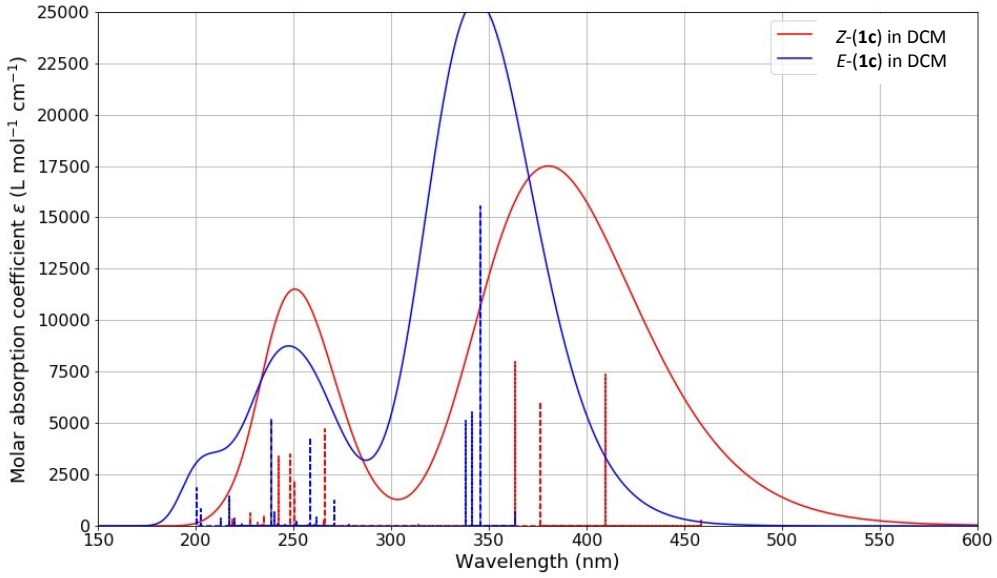

Fig. ESI46. Simulated absorption spectra for the *E* (blue) and *Z* (red) of hydrazone **1c** in dichloromethane.

HOMO-LUMO frontier orbitals

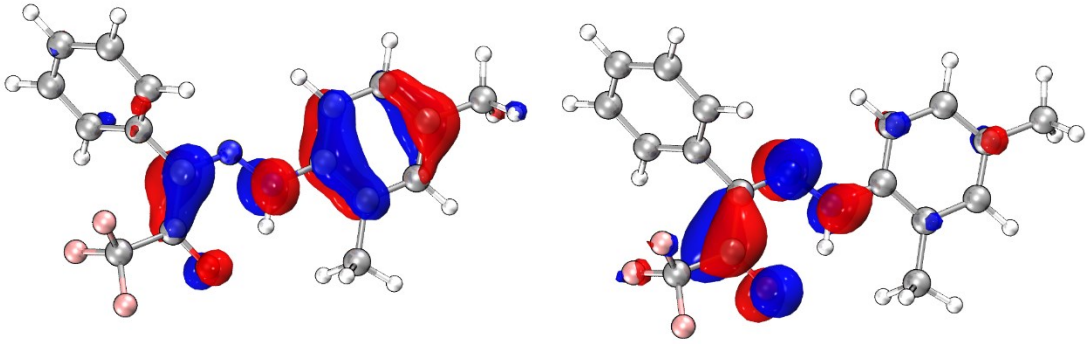

Fig. ESI47. HOMO and LUMO orbitals for (*Z*) -**1a.**

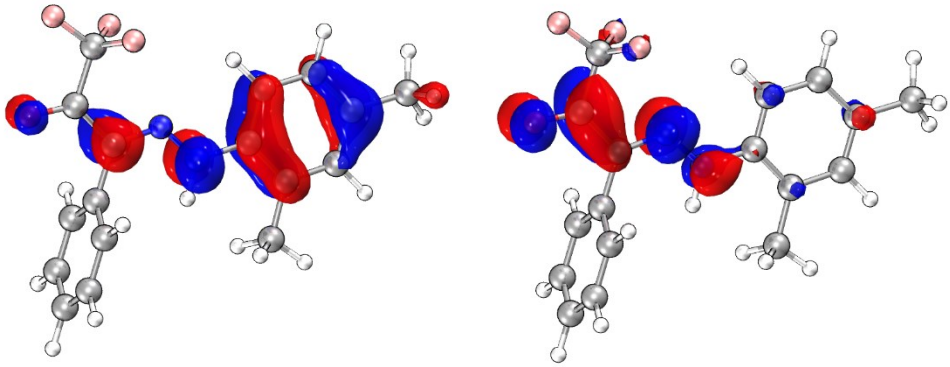

Fig. ESI48. HOMO and LUMO orbitals for (*E*) -**1a.**

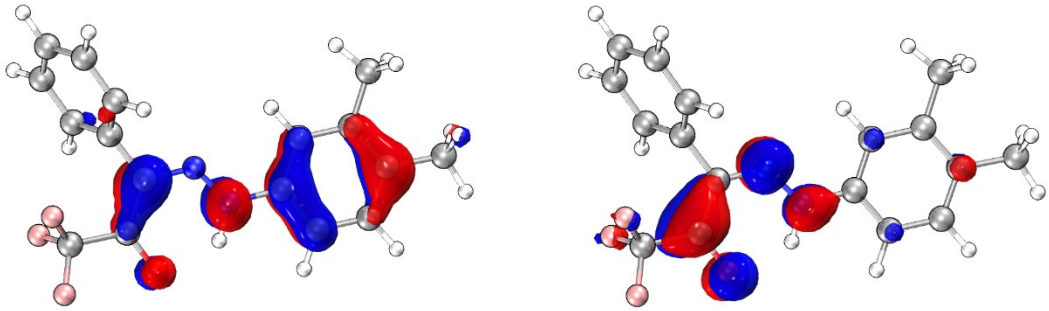

Fig. ESI49. HOMO and LUMO orbitals for (*Z*) -**1b.**

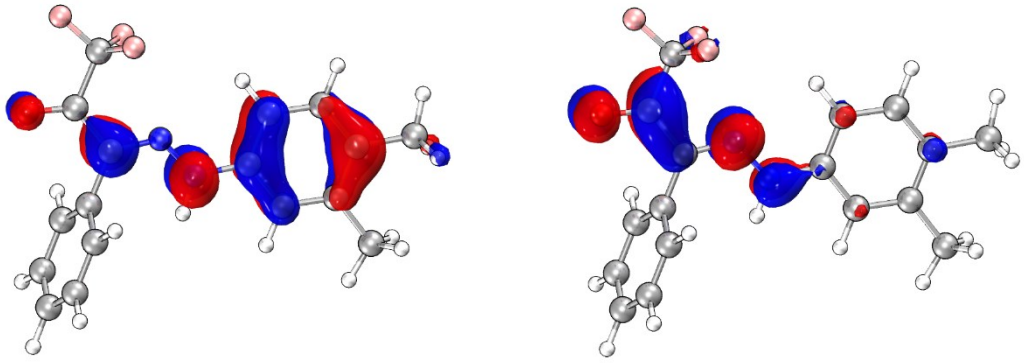

Fig ESI50. HOMO and LUMO orbitals for (*E*)-**1b.**

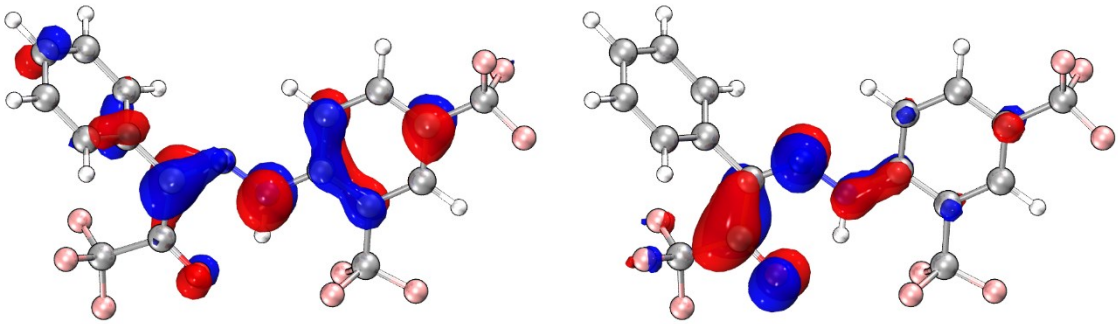

Fig. ESI51. HOMO and LUMO orbitals for (*Z*) -**1c.**

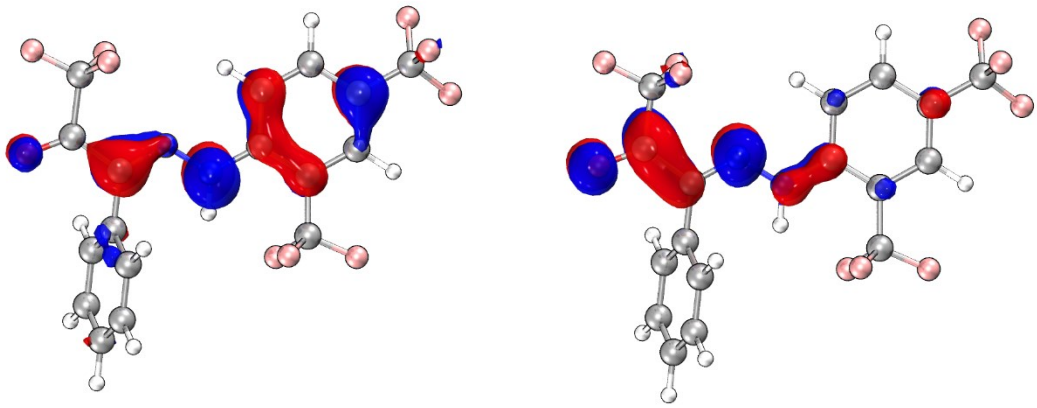

Fig. ESI52. HOMO and LUMO orbitals for (*Z*) -**1c.**

5. Kinetic studies of back thermal isomerization

A solution of hydrazone (10 mg) in $C_2D_2Cl_4$ (0.5 mL) into a NMR tube was irradiated in a Rayonet photochemical reactor equipped with UV lamps (8 x 8W) for a reaction time sufficient to have over 40% a conversion of *E* diastereoisomer into the *Z* one. Then, the reaction progressive curve of the thermal back isomerization (*Z*→*E*) was monitored by measuring a series of ^{1}H-NMR spectra (400 MHz) recorded as pseudo 2D at the temperature indicated for each sample, allowing a fixed time delay between successive spectra. Pulse width of 30° and relaxation delay of 2 seconds were used, in order to avoid errors due to the relaxation an exponential filter was applied to the FIDs for optimization of signal-to-noise ratio. Baseline correction was applied to spectra before integration. Bias and slope of integrals were carefully adjusted.

Analysis of the data points to a first-order reaction in the (*Z*) isomer concentration or (*E*) formation. The observed reaction rate constant k_{obs} (s^{-1}) was obtained by linear regression of $\ln([Z]/[Z]_0)$ *vs.* time. The activation energy barrier $\Delta G^{\ddagger}$ (kcal mol^{-1}) was calculated using the Eyring equation. The half-life time $\tau_{1/2}$ (s) was calculated by the following equation: $\tau_{1/2}=0.693/k_{obs}$.

Thermal isomerization of (*Z*)-1a into (*E*)-1a at T=300 K

k_{obs}=1.60 10^{-5} s^{-1}, $\Delta G^{\ddagger}$=24.1 kcal mol^{-1}, $\tau_{1/2}$=43321.7 s at 300 K

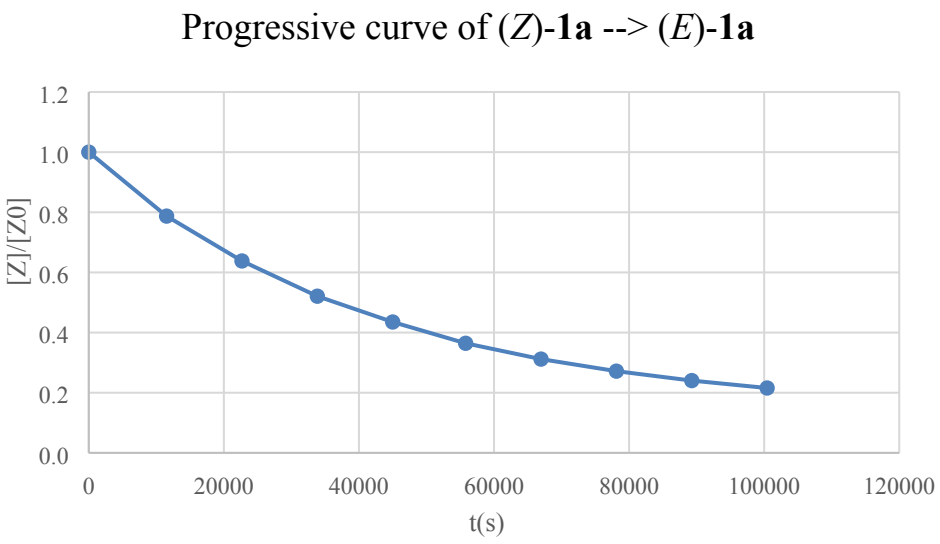

Fig. ESI53. Progressive curve for (*Z*)-**1a** into (*E*)-**1a** at T=300 K

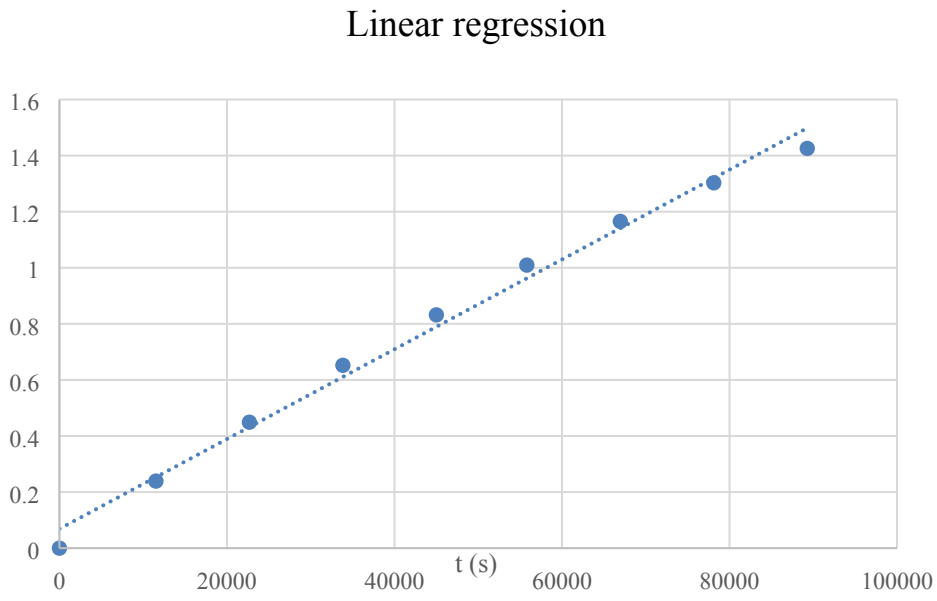

Fig. ESI54. Linear regression plot for **1a.**

Thermal isomerization of (*Z*)-1b into (*E*)-1b at T=299 K

k_{obs}=4.28 10^{-4} s^{-1}, $\Delta G^{\ddagger}$=22.1 kcal mol^{-1}, $\tau_{1/2}$=1620.7 s at 299 K

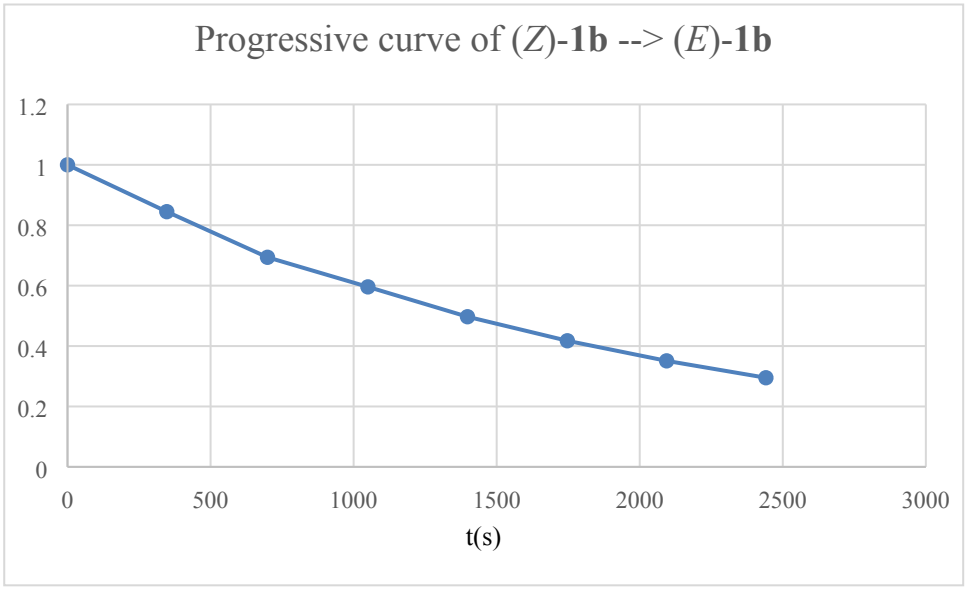

Fig ESI55. Progressive curve for (*Z*)-**1b** into (*E*)-**1b** at T=300 K

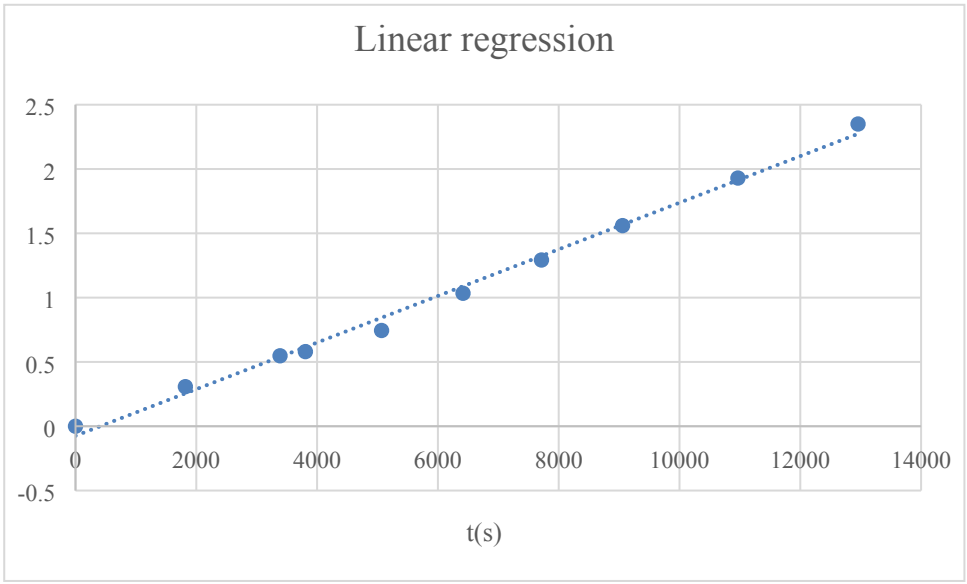

Fig. ESI56. Linear regression plot for **1b.**

Thermal isomerization of (*Z*)-1c into (*E*)-1c at T=380 K

K_{obs}=1.81 10^{-4} s^{-1}, $\Delta G^{\ddagger}$=28.9 kcal mol^{-1}, $t_{1/2}$=3829.5 s at 380 K

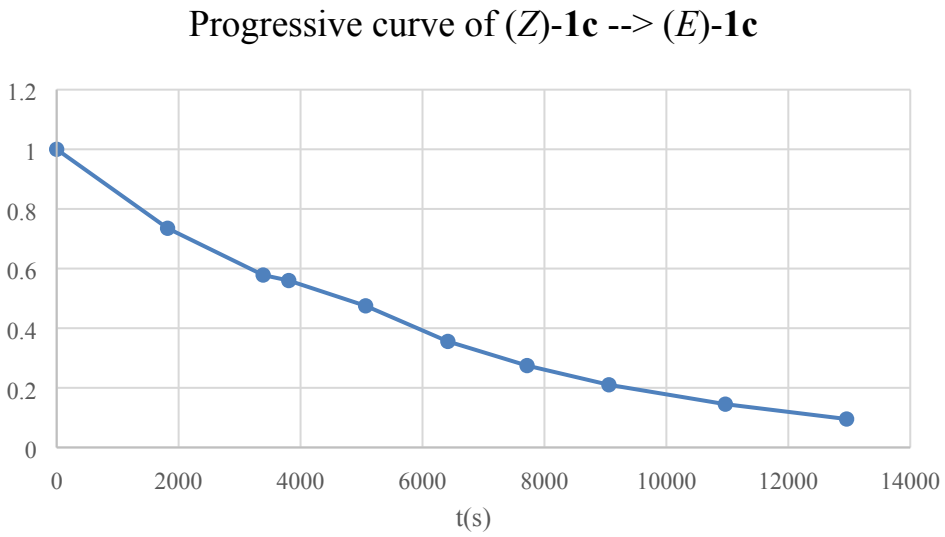

Fig. ESI57. Progressive curve for **(*Z*)-1c-> (*E*)-1c** at T=380K

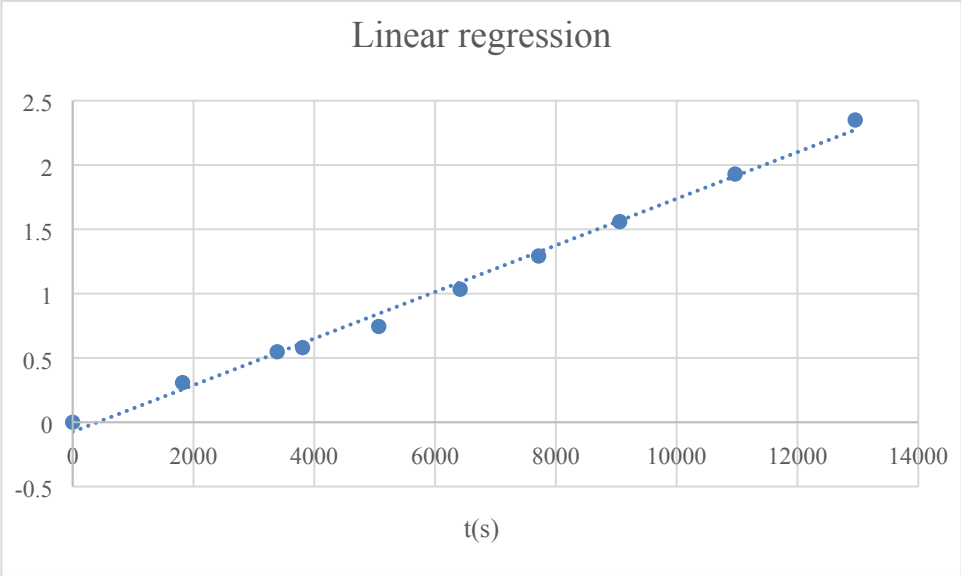

Fig. ESI58. Linear regression plot for **1c**

.

6. References

1. Dolomanov, O.V., Bourhis, L.J., Gildea, R.J, Howard, J.A.K. & Puschmann, H. (2009), J. Appl. Cryst. 42, 339-341.
2. Sheldrick, G.M. (2015). Acta Cryst. A71, 3-8.
3. Sheldrick, G.M. (2015). Acta Cryst. C71, 3-8.